PHYSICAL REVIEW B **87**, 174424 (2013)

Spinon-phonon interaction in algebraic spin liquids

Maksym Serbyn and Patrick A. Lee
Department of Physics, Massachusetts Institute of Technology, Cambridge, Massachusetts 02139, USA
(Received 8 March 2013; published 22 May 2013)

Motivated by a search for experimental probes to access the physics of fractionalized excitations called spinons in spin liquids, we study the interaction of spinons with lattice vibrations. We consider the case of algebraic spin liquid, when spinons have fermionic statistics and a Dirac-like dispersion. We establish the general procedure for deriving spinon-phonon interactions, which is based on symmetry considerations. The procedure is illustrated for four different algebraic spin liquids: π-flux and staggered-flux phases on a square lattice, π-flux phase on a kagome lattice, and zero-flux phase on a honeycomb lattice. Although the low-energy description is similar for all these phases, different underlying symmetry groups lead to a distinct form of spinon-phonon interaction Hamiltonian. The explicit form of the spinon-phonon interaction is used to estimate the attenuation of ultrasound in an algebraic spin liquid. The prospects of the sound attenuation as a probe of spinons are discussed.

DOI: 10.1103/PhysRevB.87.174424 PACS number(s): 75.10.Kt, 43.35.Bf

I. INTRODUCTION

Unambiguous experimental identification of a spin liquid,[1] an exotic ground state of a spin system in a dimension larger than one without a magnetic order, remains an open question.[2] A number of theoretical scenarios lead to a ground state with charge-neutral excitations, which carry spin-$\frac{1}{2}$ quantum number and have fermionic statistics. These excitations, called spinons, may have a Fermi surface or a Dirac spectrum,[2,3] and are usually strongly coupled to a gauge field. The latter case, so-called Dirac spin liquid phase, will be the primary subject of attention in the present paper.

Naively, one would expect that the presence of fermionic excitations in the system could be easily tested experimentally. However, measurements of different thermodynamic quantities, such as spin susceptibility or specific heat, often require subtraction and extrapolation to zero temperature, which can be ambiguous. Transport measurements are limited to a heat conductivity due to the neutral character of spinons. The heat transport measurements are difficult to perform at low temperature. Finally, neutron scattering, potentially a direct probe of spinons,[4,5] requires large single crystals which are not always available. The difficulties with experimental detection of spin liquid phases has led to a number of theoretical proposals. These include, but are not limited to, Raman scattering,[6] inelastic x-ray scattering,[7] Friedel oscillations,[8] electron spin resonance,[9] impurity physics,[10–12] and optical conductivity.[13,14]

Coupling between spinons and phonons can open additional channel of decay for phonons and change the attenuation of ultrasound. Thus, sound attenuation is another potential probe of spinons.[15] The case of spin liquid with spinon Fermi surface has been recently considered by Zhou and one of us in Ref. 16. The spinon-phonon interaction in the long wavelength limit was deduced from hydrodynamical arguments.[16–18] Assuming that electrons stay in equilibrium with lattice (due to the presence of impurities) and making canonical transformation to the moving frame, one can easily derive interaction Hamiltonian. The same interaction Hamiltonian can be reproduced from microscopical considerations using the so-called deformable ions model.[19,20]

However, as was pointed out in Ref. 16, spinons with a Dirac spectrum require a different treatment. Here we address this problem and consider the contribution of spinons to the attenuation of ultrasound in a Dirac spin liquid. Contrary to the case of electrons[18–20] or spinons with Fermi surface,[16] it appears that there is no universal form for the interaction of spinons with acoustic phonons in Dirac spin liquid. This is related to the spinor nature of spinons with Dirac dispersion. Similarly to graphene, spinor structure describes the character of wave function on different sublattices, i.e., on the microscopic scale. Consequently, one possible route of deducing the form of spinon-phonon interaction would be to find the change of the Hamiltonian of the spinons induced by the long wave modulation of the lattice parameters, starting from a microscopic Hamiltonian. This procedure, although giving explicit values of coupling constants, is not universal. It depends on the microscopic implementation of a different spin liquid phase. Moreover, it is difficult to guarantee that one finds all possible terms in the interaction Hamiltonian.

We adopt a different approach and use symmetry considerations to find a spinon-phonon interaction Hamiltonian. A similar route has been recently used to deduce electron-phonon interaction in graphene.[21,22] There, representations of the lattice symmetry group of the honeycomb lattice on continuous Dirac fields were used to find all possible symmetry-allowed electron-phonon couplings.[22] However, in a Dirac spin liquid, also referred to as an algebraic spin liquid, the notion of symmetry group has to be extended to the projective symmetry group.[23,24]

In this paper we generalize the derivation of spinon-phonon interaction Hamiltonian to the case of projective representation of lattice symmetry group. The procedure is straightforward, and it requires studying the representation of symmetry group on spin-singlet fermionic bilinears. We consider four different realizations of the Dirac spin liquid: π-flux[25] and staggered-flux[26] phases on a square lattice, as well as π-flux phase on a kagome lattice[27] and a Dirac spin liquid phase on a honeycomb lattice. Within low-energy effective field theory, all these phases can be described in terms of Dirac excitations, coupled to a gauge field.[25–31] Nevertheless, these phases retain the information about their microscopic origin. This information

is encoded in the projective representation of spinon operators under the action of the corresponding symmetry group.

As we see below, the projective character of the representation of symmetry group has a profound consequences on a spinon-phonon interaction. For all algebraic spin liquid phases considered here except for the Dirac spin liquid on a honeycomb lattice, only the coupling to the density of spinons is allowed by symmetry at the leading order. However, we find that this coupling is screened due to the gauge field. The sound attenuation coming from the next order terms is suppressed by an extra factor and behaves as T^3 at low temperatures. In contrast, the Dirac spin liquid on a honeycomb lattice has a sound attenuation $\propto T$. Although the sound attenuation in all cases is suppressed compared to the case of a spin liquid with a Fermi surface, the spinon contribution is still the dominant process at low temperature and experimental observation of the attenuation of ultrasound due to spinons may be possible.

The paper is organized as follows. Section II introduces the low-energy description of Dirac spin liquid and projective symmetry group. We use the π-flux phase on a square lattice as an example. Next, we discuss interaction of spinons with phonons in Sec. III. We describe the general procedure of obtaining a spinon-phonon interaction Hamiltonian from symmetry considerations. It is later illustrated in more detail for the π-flux phase on a square lattice. Having found the interaction Hamiltonian, in Sec. IV we study the sound attenuation, concentrating on attenuation of longitudinal sound. Finally, in Sec. V we summarize and discuss our results. Basic facts from the representation theory of finite groups and details on the calculation of sound attenuation are given in Appendixes.

II. LOW-ENERGY DESCRIPTION OF ALGEBRAIC SPIN LIQUIDS

We review the description of algebraic spin liquid fixed point using the language of low-energy effective field theory.[25–31] This description suits our purposes since we are interested in coupling between acoustic phonons in the low energy limit. In addition, it provides a universal framework applicable to a variety of different algebraic spin liquid phases. In short, three ingredients are needed in order to specify a low-energy field description of a given algebraic spin liquid phase. These are a low-energy Hamiltonian for continuous fields, a gauge group, and a representation of projective symmetry group specified by its action on fields. Below we review these ingredients for the general case, as well as illustrate them for the π-flux phase on a square lattice (πF$\square$ phase). We do not list details for the staggered flux phase on a square lattice (sF$\square$), π-flux phase on a kagome lattice (πF$\hexagon$), and Dirac spin liquid phase on a honeycomb lattice (0F$\bigcirc$). The reader is referred to Refs. 25–27 for more details specific for these phases.

A. Effective field theory, gauge group, and projective symmetry group

The starting point is the spin $S = 1/2$ model on some (not necessarily Bravais) two-dimensional lattice. The symmetries of spin Hamiltonian are assumed to include SU(2) spin rotations, time reversal, and the full lattice group of a given lattice. We write the Hamiltonian as

$$H = \sum_{\langle ij \rangle} J_{ij} \boldsymbol{S}_i \cdot \boldsymbol{S}_j + \cdots, \tag{1}$$

where bold indices $\boldsymbol{i}, \boldsymbol{j}$ denote lattice sites and the sum goes over nearest-neighbor pairs of sites. The ellipsis denotes other short-range interaction terms required to stabilize the required spin liquid phase.

In order to get access to phases with no spin order, we use slave-fermion mean-field theory. We represent spin operators using spinon operators $f_{i,\alpha}, \alpha = \uparrow, \downarrow$:

$$\boldsymbol{S}_i = \tfrac{1}{2} f^\dagger_{i\alpha} \boldsymbol{\sigma}_{\alpha\beta} f_{j\beta}. \tag{2}$$

The mapping between Hilbert spaces is exact, provided one imposes a constraint of no double occupancy, $f^\dagger_{i\alpha} f_{i\alpha} = 1$, where summation over repeating indices is implied. Such representation of spin has SU(2) gauge redundancy. Therefore, mean-field decoupling of spin interaction has to include a SU(2) gauge field on the links of the lattice. Saddle points of the mean-field theory, depending on their structure,[23,24] may break this SU(2) symmetry down to U(1) or $\mathbb{Z}_2$.

We are mostly interested in phases with U(1) gauge symmetry [the only SU(2)-symmetric algebraic spin liquid phase considered here is the πF$\square$ phase[24]]. General lattice gauge theory Hamiltonian at the saddle point is

$$H_{\mathrm{U(1)}} = \frac{h}{2} \sum_{\langle ij \rangle} e^2_{ij} - K \sum_{\text{plaq.}} \cos(\phi_\square) + \sum_{\langle ij \rangle} [\chi_{ji} e^{-i a_{ji}} f^\dagger_{i\alpha} f_{j\alpha} + \text{H.c.}], \tag{3}$$

where we assume that the choice of χ_{ij} leads to a Dirac spectrum. The gauge redundancy leads to the appearance of a_{ij}, a compact U(1) vector potential living on the bonds of the lattice, and e_{ij}, which is canonically conjugate electric field taking integer values. We also defined $\phi_\square$, living on the dual lattice, as the lattice version of the curl of gauge field a_{ij}. The gauge constraint is $(\mathrm{div}\, e)_i + f^\dagger_{i\alpha} f_{i\alpha} = 1$. Although initially the vector potential does not have any kinetic terms, these will be generated due to coupling with fermions and are written in Eq. (3) with coefficient K. For $K = 0$, $h \gg |\chi_{ij}|$, one recovers the spin model from Eq. (3). Mean field is a good approximation when $K \gg |\chi_{ij}| \gg h$ and describes the algebraic spin liquid phase. It has been argued that this phase is stable.[25,26] Monopoles are irrelevant, leading to the gauge group becoming noncompact in the low-energy limit. Therefore, it should be accessible starting from the spin Hamiltonian in Eq. (1) for some range of initial parameters. More detailed discussions of stability of algebraic spin liquid phase are presented in Refs. 25 and 26.

Provided that the choice of χ_{ij} leads to a Dirac spectrum, we use continuous fermionic fields to write the low-energy Hamiltonian. In the momentum space it reads

$$H = v_F \int \frac{d^2 \boldsymbol{k}}{(2\pi)^2} \psi^\dagger_{\sigma a \alpha} [(\boldsymbol{k} - \boldsymbol{a}) \cdot \boldsymbol{\tau}_{\alpha\beta}] \psi_{\sigma a \beta}. \tag{4}$$

The indices σ, a, and α in a continuous eight-component fermion field $\psi_{\sigma a \alpha}$ label spin, Dirac valley, and sublattice, respectively. In what follows, we use three different sets of

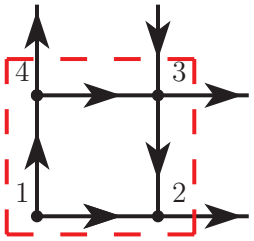

FIG. 1. (Color online) Choice of the ansatz for the πF$\square$ phase. The red dashed line encloses the unit cell. Numbers indicate the labeling of sites used in the main text. Hopping in the direction of the arrows is proportional to $+i$.

Pauli matrices acting in different spaces. Pauli matrices acting on the spin indices are denoted as $\{\sigma^x,\sigma^y,\sigma^z\}$. The second index distinguishes between different Dirac points (valleys) and we label Pauli matrices acting in this space as $\{\mu^x,\mu^y,\mu^z\}$. Finally, Eq. (4) involves Pauli matrices $\{\tau^x,\tau^y,\tau^z\}$ acting on spinor (sublattice) indices. Below we omit the sign of the tensor product, implying, e.g., $\sigma^y\tau^x = \sigma^y \otimes \mathbb{1} \otimes \tau^x$.

A particular choice of ansatz χ_{ij} naively violates some symmetries of the original Hamiltonian. However, representation Eq. (2) is invariant under the gauge transformations

$$f_i \to f_i e^{i\theta_i}, \quad a_{ij} \to a_{ij} + \theta_i - \theta_j. \tag{5}$$

Consequently, there is a freedom in the choice of the action of different symmetries: One can supplement them with some gauge transformation. Requiring mean field Hamiltonian (3) to remain invariant we can fix this freedom and show that all symmetries of original spin Hamiltonian remain unbroken.

The fact that the action of symmetries on fermionic fields is supplemented by gauge transform has a deep consequences. Rather than forming the usual representation of lattice symmetry group, fermions are said to realize *projective representation* of lattice symmetry group.[23,24] This representation is fully specified by the action of the lattice symmetry group generators on the fermionic fields. Knowing the mapping from the lattice fields $f_{i\alpha}$ to ψ, one can easily find the action of generators on the continuous fermionic field. Below, we demonstrate this procedure for the πF$\square$ phase.

B. Example: π-flux spin liquid on a square lattice

We use the the πF$\square$ phase[25] to illustrate the abstract construction presented above. The starting point is the choice-specific values of χ_{ij} in Eq. (3) to fix the mean-field ansatz. Our notations are different from those in Ref. 25. We quadruple our unit cell, so it includes four sites. Sites within the new unit cell are labeled by an index $m = 1,\ldots,4$ as in Fig. 1. The χ_{ij} and a_i^0 are chosen as

$$\chi_{ii+\hat{x}} = i, \quad \chi_{ii+\hat{y}} = (-)^{i_x} i; \quad a_i^0 = 0. \tag{6}$$

The resulting mean-field Hamiltonian with the spin index and gauge field omitted is

$$H_{\rm mf} = -\frac{1}{2}J\sum_{\boldsymbol{r}}\big[i(f_{\boldsymbol{r}2}^\dagger + f_{\boldsymbol{r}4}^\dagger)f_{\boldsymbol{r}1} + i\big(f_{\boldsymbol{r}3}^\dagger + f_{\boldsymbol{r}+\boldsymbol{a}_2 1}^\dagger\big)f_{\boldsymbol{r}4} + i\big(f_{\boldsymbol{r}+\boldsymbol{a}_1 1}^\dagger - f_{\boldsymbol{r}3}^\dagger\big)f_{\boldsymbol{r}2} + i\big(f_{\boldsymbol{r}+\boldsymbol{a}_1 4}^\dagger - f_{\boldsymbol{r}+\boldsymbol{a}_2 2}^\dagger\big)f_{\boldsymbol{r}3} + \text{H.c.}\big], \tag{7}$$

where the Bravais lattice vector $\boldsymbol{r} = n_1\boldsymbol{a}_1 + n_2\boldsymbol{a}_2$, with n_1, n_2 integers labeling unit cells, and $\boldsymbol{a}_1 = 2\hat{\boldsymbol{x}}$, $\boldsymbol{a}_2 = 2\hat{\boldsymbol{y}}$. Making Fourier transform

$$f_{\boldsymbol{r}m} = \frac{1}{\sqrt{N}}\sum_{\boldsymbol{k}} e^{i\boldsymbol{k}\cdot\boldsymbol{r}} f_{\boldsymbol{k}m}, \tag{8}$$

where N is the number of unit cells, we obtain the Hamiltonian in momentum space

$$H_{\rm mf} = -\frac{J}{2}\sum_{\boldsymbol{k}} f_{\boldsymbol{k}m}^\dagger H_{mn}(\boldsymbol{k}) f_{\boldsymbol{k}n}, \tag{9}$$

where the 4×4 matrix $H(\boldsymbol{k})$ is given by

$$H_{mn}(\boldsymbol{k}) = i\begin{pmatrix} 0 & -1+K_1^* & 0 & -1+K_2^* \\ 1-K_1 & 0 & 1-K_2^* & 0 \\ 0 & -1+K_2 & 0 & 1-K_1 \\ 1-K_2 & 0 & -1+K_1^* & 0 \end{pmatrix}, \tag{10}$$

with the notation $K_{1,2} = e^{i\boldsymbol{k}\cdot\boldsymbol{a}_{1,2}}$. The momentum is measured in the units of the inverse lattice constant of the original lattice (i.e., before enlarging the unit cell), which is set to one in what follows. We choose the Brillouin zone as $k_x, k_y \in [-\pi/2,\pi/2)$. The energy levels of the Hamiltonian (9) and (10) are doubly degenerate. Therefore, there is only one doubly degenerate gapless Fermi point in the Brillouin zone, which is located at the momentum $\boldsymbol{Q} = (0,0)$. In the vicinity of this point the dispersion is described by Dirac fermions and we can define continuum fermion fields. We choose the following representation for two copies of spinor field $\psi_{a\alpha}(\boldsymbol{k})$:

$$\psi_1(\boldsymbol{k}) \sim \frac{1}{\sqrt{2}}\begin{pmatrix} if_{\boldsymbol{k}2} + f_{\boldsymbol{k}4} \\ -if_{\boldsymbol{k}1} - f_{\boldsymbol{k}3} \end{pmatrix}, \tag{11a}$$

$$\psi_2(\boldsymbol{k}) \sim \frac{1}{\sqrt{2}}\begin{pmatrix} f_{\boldsymbol{k}1} + if_{\boldsymbol{k}3} \\ -f_{\boldsymbol{k}2} - if_{\boldsymbol{k}4} \end{pmatrix}, \tag{11b}$$

where the index $a = 1,2$ labels different Dirac points, $K_\pm$, both located at the Γ point of the Brillouin zone. Consequently, the low-energy continuum Hamiltonian is written as

$$H_{\rm Dirac} = v_F\int\frac{d^2\boldsymbol{k}}{(2\pi)^2}\psi_{\sigma a}^\dagger(k_x\tau^x + k_y\tau^y)\psi_{\sigma a}, \tag{12}$$

where we made spinor index implicit. Fermi velocity, provided the lattice constant is set to one, coincides with J, $v_F = J$.

The continuous fields $\psi_{a\alpha}(\boldsymbol{k})$ realize a projective representation of the lattice symmetry group. This representation is fully specified if one knows the action of group generators on continuous fields. The relevant lattice symmetry group in this case, denoted as C_{4v}', is different from the point symmetry group of square C_{4v} due to an enlarged unit cell. Consequently, the group C_{4v}', in addition to elements from C_{4v}, contains translations by unit vectors of square lattice along x and y axes. The full set of generators, the action of which is to be specified below, contains rotation for angle $\pi/2$, $\mathcal{R}_{\pi/2}$, reflection of the x axis, $\mathcal{R}_x$ (these are generators of C_{4v}), and lattice translation by vector $\boldsymbol{a}_1$, T_x. In addition, we also have to specify the action of time-reversal symmetry, $\mathcal{T}$, and charge conjugation operators, $\mathcal{C}$.

Let us illustrate the derivation of the action of reflection generator on the continuous fields. The action of $\mathcal{R}_x$ on the unit cell may be symbolically shown as

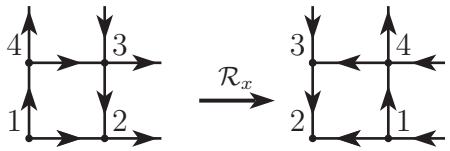

(13)

From here we can understand the action of $\mathcal{R}_x$ on the lattice fermion fields as exchanging fermionic operators with indices $1 \leftrightarrow 2$ and $3 \leftrightarrow 4$. However, in order to leave Hamiltonian (7) invariant, this has to be supplemented by gauge transform that changes the sign of all hoppings [thus reversing the direction of all arrows in the right-hand side of Eq. (13)]. One can easily check that transformation

$$f_{\boldsymbol{r}1} \to f_{\boldsymbol{r}'2}, \quad f_{\boldsymbol{r}2} \to -f_{\boldsymbol{r}'1}, \tag{14a}$$

$$f_{\boldsymbol{r}3} \to f_{\boldsymbol{r}'4}, \quad f_{\boldsymbol{r}4} \to -f_{\boldsymbol{r}'3}, \tag{14b}$$

$$\boldsymbol{r}' = \mathcal{R}_x \boldsymbol{r} = (-r_x, r_y), \tag{14c}$$

leaves Hamiltonian (7) invariant. The action of $\mathcal{R}_x$ on operators $f_{\boldsymbol{r}n}$ is easy to translate into the representation of $\mathcal{R}_x$ on the continuous fermionic fields using their definition (11). In terms of different sets of Pauli matrices introduced above, it can be written as

$$\psi \to \mathcal{R}_x \psi \quad \text{with} \quad \mathcal{R}_x = i\mu^z \tau^y. \tag{15}$$

Using an analogous procedure we get the representation of the remaining generators to be

$$\mathcal{R}_{\pi/2} = \tfrac{1}{2}(\mu^x + \mu^y)(1 + i\tau^z), \tag{16}$$

$$T_x = \mu^y. \tag{17}$$

Finally, for the π-flux phase there exist two additional SU(2) transformations not related to lattice symmetry group. These are time reversal, $\mathcal{T}$, defined as an antiunitary operator which flips the direction of spin operator (2), and charge conjugation, $\mathcal{C}$. The latter operation may be viewed as a SU(2) rotation in the spin space by π around y axis,[25] supplemented by the particle-hole transformation. On the lattice level (in momentum space) these can be conveniently represented by

$$\mathcal{T}: \quad f_{\boldsymbol{k}\sigma 1,3} \leftrightarrow f^\dagger_{\boldsymbol{k}\sigma 1,3}, \quad f_{\boldsymbol{k}\sigma 2,4} \leftrightarrow -f^\dagger_{\boldsymbol{k}\sigma 2,4}, \tag{18a}$$

$$\mathcal{C}: \quad f_{\boldsymbol{k}\uparrow n} \to f^\dagger_{-\boldsymbol{k}\downarrow n}, \quad f_{\boldsymbol{k}\downarrow n} \to -f^\dagger_{-\boldsymbol{k}\uparrow n}, \tag{18b}$$

where $\mathcal{T}$ reversal also includes complex conjugation operation, and spin indices were restored. Although these definitions may look counterintuitive, one can check that the charge conjugation (18b) indeed leaves the spin operator invariant, whereas the time-reversal symmetry, defined as in Eq. (18a), flips the direction of the spin operator in Eq. (2). Mapping this action to continuous fermionic fields, we have

$$\mathcal{T}: \quad \psi \to \mu^z \tau^z (\psi^\dagger)^T, \tag{19a}$$

$$\mathcal{C}: \quad \psi \to (i\sigma^y)(i\mu^x \tau^x)(\psi^\dagger)^T. \tag{19b}$$

As we pointed out earlier, the representation of the lattice symmetry group on fermions is projective. This can be easily seen from the action of generators, Eqs. (15)–(17), if one tries to test some group identities. For example, $(\mathcal{R}_{\pi/2})^4$ is a trivial transformation. However, using the explicit form of the representation of $\mathcal{R}_{\pi/2}$ for continuous fermionic fields, Eq. (16), we find

$$(\mathcal{R}_{\pi/2})^4 = -\mathbb{1}. \tag{20}$$

Thus, all group identities hold only up to some gauge transformation, which leaves the Hamiltonian invariant.

III. SPINON-PHONON INTERACTION

Having a low-energy description of Dirac spin liquid phases at our disposal, in this section we consider the spinon-phonon interaction.

As we explained in the Introduction, the hydrodynamic approach,[16–18] applicable for the case of spin liquid with the Fermi surface, is not straightforward to use in our case. It is the presence of spinor structure, inherently related to the microscopic details such as two inequivalent sublattices, that prevents application of hydrodynamical arguments. Of course, one can always resort to the microscopic derivation of spinon-phonon interaction. Despite the advantage of giving specific values of coupling constants, this route is highly nonuniversal and is not guaranteed to yield all possible couplings.

We present a universal procedure for finding all possible terms in a spinon-phonon interaction Hamiltonian allowed by symmetry. First, we introduce phonons and the general form of the spinon-phonon interaction Hamiltonian. After this the general idea behind the procedure is described. Implementation of this procedure for the πFD phase serves as an example. Finally, we present results for other Dirac spin liquid phases and discuss the underlying physics. The derivation of these results relies extensively on a representation theory for finite groups. Necessary concepts, as well as basic facts about point groups of square, kagome, and honeycomb lattices, are listed in Appendix A.

A. Spinon-phonon interaction Hamiltonian from symmetry considerations

We start with specifying conventions for the spinon-phonon interaction Hamiltonian. It is written using the operator $\hat{H}_{\text{s-ph}}(\boldsymbol{k},\boldsymbol{q})$ as

$$\mathcal{H}_{\text{s-ph}} = \sum_{\boldsymbol{k},\boldsymbol{q}} \psi^\dagger(\boldsymbol{k}+\boldsymbol{q}) \hat{H}_{\text{s-ph}}(\boldsymbol{k},\boldsymbol{q}) \psi(\boldsymbol{k}). \tag{21}$$

In what follows we refer to the operator $\hat{H}_{\text{s-ph}}(\boldsymbol{k},\boldsymbol{q})$ itself as a spinon-phonon interaction Hamiltonian. Normally, the operator $\hat{H}_{\text{s-ph}}(\boldsymbol{k},\boldsymbol{q})$ obtained from the procedure described above, would contain only zeroth-order terms in the distance from the Dirac point, $\boldsymbol{k}$, $\hat{H}_{\text{s-ph}}(\boldsymbol{k},\boldsymbol{q}) = \hat{H}_{\text{s-ph(0)}}(\boldsymbol{q})$. As we shall see, in some cases, all such terms vanish. Then, to find a nonzero interaction Hamiltonian, we allow the presence of terms, linear in $\boldsymbol{k}$, $\hat{H}_{\text{s-ph(1)}}(\boldsymbol{k},\boldsymbol{q})$ and the total Hamiltonian will be written as a sum:

$$\hat{H}_{\text{s-ph}}(\boldsymbol{k},\boldsymbol{q}) = \hat{H}_{\text{s-ph(0)}}(\boldsymbol{q}) + \hat{H}_{\text{s-ph(1)}}(\boldsymbol{k},\boldsymbol{q}). \tag{22}$$

In what follows, we restrict ourselves to the first nonvanishing term in this expansion. Phonons enter $\hat{H}_{\text{s-ph}}(\boldsymbol{k},\boldsymbol{q})$ via the $\boldsymbol{q}$ Fourier component of displacement field, $\boldsymbol{u}(t,\boldsymbol{r})$. In the second

quantized language the displacement field is written as

$$\boldsymbol{u}(t,\boldsymbol{r}) = \sum_{\boldsymbol{q},\mu} \sqrt{\frac{\hbar}{2S\rho\omega_{\boldsymbol{q}}}} \boldsymbol{e}_{\boldsymbol{q}\mu} (a_{\boldsymbol{q}\mu} e^{-i\omega_{\boldsymbol{q}}t + i\boldsymbol{q}\cdot\boldsymbol{r}} + a^{\dagger}_{-\boldsymbol{q}\mu} e^{i\omega_{\boldsymbol{q}}t - i\boldsymbol{q}\cdot\boldsymbol{r}}), \tag{23}$$

where index $\mu = \mathrm{L,T}$ labels longitudinal and transverse modes of acoustic phonons, and $\boldsymbol{e}_{\boldsymbol{q}\mu}$ is the corresponding polarization vector. The dispersion of phonons is assumed in the form $\omega_{\boldsymbol{q}} = v_s|\boldsymbol{q}|$, where v_s is the sound velocity. The ρ is defined as a mass density per layer, and S is the area. For simplicity we consider only in-plane phonon modes.

Although we work in a continuum limit, it is the lattice symmetry group and its representations that determine the properties of low-energy (acoustic) phonons and spinon excitations. Phonons are described using vector $\boldsymbol{u}(t,\boldsymbol{r})$, specifying displacement at a given point $\boldsymbol{r}$ due to deformation. As a uniform displacement of the entire lattice, $\boldsymbol{u}(t,\boldsymbol{r}) = \boldsymbol{u}_0$, leaves a system invariant, acoustic phonons can couple to spinons only via spatial derivatives of $\boldsymbol{u}(\boldsymbol{r})$ (we ignore coupling to the time derivative, as it is suppressed by the ratio of sound to Fermi velocities). The set of all spatial derivatives, $\partial_i u_j(\boldsymbol{r})$ or $-iq_i u_j(\boldsymbol{q})$, in the Fourier space transforms as a rank 2 tensor under the lattice symmetry group. Representation of a lattice symmetry group on a rank 2 tensor can be split as a sum of irreducible representations. Symbolically, this is written as

$$E_1 \times E_1 = \sum_j \oplus D^{\mathrm{ph}}_j, \tag{24}$$

where E_1 is vector representation and D^{ph}_j are (possibly repeating) irreducible representations. Acoustic phonon modes can be classified using irreducible components, present in this decomposition.

Spinons have fermionic statistics; thus, minimal coupling to phonons must involve bilinears of ψ field. Contrary to phonons, continuous spinon fields ψ realize *projective* representation of the lattice symmetry group. The action of lattice symmetries on ψ, in general, includes the gauge transformation, and all identities between generators are valid modulus gauge transformation [for example, see Eq. (20)]. Similar to a single field ψ, a general spinon bilinear also realizes projective representation of the lattice symmetry group. However, there exists a *subset* of spinon bilinears which transform under regular representation of symmetry group. For the case when the gauge group is SU(2) these are bilinears which are singlets under SU(2), whereas for Abelian gauge groups, like U(1) or $\mathbb{Z}_2$, *all* bilinears realize regular representation, as gauge components cancel.

Regular representation of the lattice symmetry group on (a subset of) spinon bilinears can be split into irreducible representations $D^{\psi^\dagger\psi}_j$,

$$G_{\psi^\dagger\psi} = \sum_j \oplus D^{\psi^\dagger\psi}_j. \tag{25}$$

We note that invariant fermionic bilinears for πF$\square$, sF$\square$, and πF$\hexagon$ phases were identified in Refs. 25–27. This corresponds to finding all trivial components contained within decomposition (25).

The product of two irreducible representations, $D^{\mathrm{ph}}_i \times D^{\psi^\dagger\psi}_j$ contains a trivial representation within itself if and only if these representations coincide, $D^{\mathrm{ph}}_i \equiv D^{\psi^\dagger\psi}_j$. As the spinon-phonon interaction Hamiltonian has to be invariant under the action of the symmetry group, we can construct all symmetry-allowed couplings by pairing identical irreducible components between splittings (24) and (25). The presence of additional symmetry operations, such as time reversal or charge conjugation, may impose further restrictions on the obtained set.

B. Example: Derivation for the π-flux phase

We use the πF phase as an example for an illustration of the abstract procedure outlined above. For phonons, the underlying symmetry group is C_{4v} (see Appendix A 2). Using characters Table V, we find explicit form of the decomposition (24) for the present case:

$$E_1 \times E_1 = A_1 \oplus A_2 \oplus B_1 \oplus B_2. \tag{26}$$

A_1 here and in what follows always denotes the trivial representation. All other representations are also one-dimensional; thus the action of corresponding group elements can be inferred from Table V in Appendix A. In terms of components of two vectors (q_x,q_y) and (u_x,u_y), the basis functions of these representations are

$$A_1 : u_{xx} + u_{yy}, \quad A_2 : u_{xy} - u_{yx}, \tag{27a}$$

$$B_1 : u_{xx} - u_{yy}, \quad B_2 : u_{xy} + u_{yx}, \tag{27b}$$

where we used shorthand notation

$$u_{ij} \equiv q_i u_j. \tag{28}$$

While introducing the ansatz for the πF$\square$ phase in Sec. II B we used a unit cell consisting of four lattice sites. This allowed us to write relations between continuous fields and microscopic spinon operators in a simple form. However, the price to pay is that spinons now transform under the symmetry group C'_{4v} which is larger than point symmetry group of the square lattice. In addition to transformations from the point group of the square C_{4v}, group C'_{4v} includes lattice translations by unit vector in the $\hat{x}$ and $\hat{y}$ directions. The details about irreducible representations of group C'_{4v} are worked out in Appendix A 2. It has eight one-dimensional irreducible representations, labeled as $A_{1,2}, B_{1,2}$ and $A'_{1,2}, B'_{1,2}$ in Table VII, and six two-dimensional representations, denoted as $E_1, E'_1, E_{2,\ldots,5}$. To find the splitting of representation of C'_{4v} on spinon bilinears into irreducible components we use a natural basis: All spin singlet bilinears can be enumerated using tensor products of Pauli matrices acting in sublattice and valley space,

$$\psi^\dagger M \psi, \quad M \in \{\mathbb{1}, \tau^i, \mu^i, \tau^i\mu^j\}. \tag{29}$$

With the help of the characters Table VII, the 16-dimensional representation $G^{\pi F}_{\psi^\dagger\psi}$ is reduced into direct sum of four one-dimensional and six two-dimensional representations as

$$G^{\pi\mathrm{F}}_{\psi^\dagger\psi} = A_1 \oplus A_2 \oplus B'_1 \oplus B'_2 \oplus E_1 \oplus E'_1 \oplus E_2 \oplus E_3 \oplus E_4 \oplus E_5. \tag{30}$$

TABLE I. Explicit form of basis in terms of tensor products of Pauli matrices for irreducible representations of C'_{4v} contained within $G^{\pi F}_{\psi^\dagger\psi}$. The last two rows show properties of basis elements under time reversal and charge conjugation. Pluses imply invariance, whereas minuses indicate a change of sign under the action of corresponding symmetry.

Representation	A_1	A_2	B'_1	B'_2	E_1	E_2	E'_1	E_3	E_4	E_5
Basis	$\mathbb{1}$	τ^z	μ^z	$\mu^z\tau^z$	τ^x,τ^y	μ^x,μ^y	$\mu^z\tau^x,\mu^z\tau^y$	$\mu^x\tau^z,\mu^y\tau^z$	$\mu^x\tau^y,\mu^y\tau^x$	$\mu^x\tau^x,\mu^y\tau^y$
$\mathcal{T}$-inv	$-$	$-$	$-$	$-$	$+$	$+$	$+$	$+$	$-$	$-$
$\mathcal{C}$-inv	$-$	$+$	$+$	$-$	$-$	$-$	$+$	$+$	$-$	$-$

Using the explicit basis (29), we can find to what irreducible representation a given matrix belongs. Identity matrix $\mathbb{1}$ corresponds to the trivial representation, A_1. Next, one can check that both matrices μ^z, τ^z, and their product, $\mu^z\tau^z$, are invariant (up to a sign) under the action of all generators of C'_{4v} [Eqs. (15)–(17)]. Therefore, the matrices μ^z, τ^z, and $\mu^z\tau^z$ form the basis of one-dimensional representations A_2, B'_1, and B'_2, respectively. Matrices (τ^x,τ^y), $(\mu^z\tau^x,\mu^z\tau^y)$, and (μ^x,μ^y) constitute the basis of two-dimensional irreducible representations E_1, E'_1 and E_2, respectively. Finally, after some algebra, the remaining six matrices from (29) can be split into pairs that realize the basis for representations $E_3,\dots,E_5$ as shown in Table I. The last two rows in Table I display the symmetry of corresponding matrices under the action of time reversal and charge conjugation operations.

Explicit decompositions, Eqs. (26) and (30), give us allowed couplings between spinons and phonons. Only identical irreducible representations can be coupled between themselves. Comparing Eqs. (26) and (30) we see that only two first terms in both direct sums coincide. Thus, one may expect the allowed couplings to be described by contraction between A_1 (A_2) components in different sums. However, according to Table I, the bilinear $\psi^\dagger\mathbb{1}\psi$ is odd under both time reversal and charge conjugation, and $\psi^\dagger\tau^z\psi$ is odd under time reversal. As different components of u_{ij} are invariant under time-reversal and charge conjugation, we conclude that at the leading order no couplings of spinons to phonons are allowed by symmetry, $\hat{H}^{\pi\mathrm{F}\square}_{\text{s-ph(0)}}(\boldsymbol{q}) = 0$.

To find a nonzero coupling of spinons to phonons, we allow for the presence of spinon momentum, $\boldsymbol{k}$ in the coupling Hamiltonian. This corresponds to the next order in the expansion around the Dirac points. The spinon momentum, $\boldsymbol{k}$, transforms under the usual vector representation E_1 [this can be inferred from the fact that the Dirac Hamiltonian, Eq. (12), is invariant] and is invariant under time reversal, but odd under charge conjugation. The product $E_1 \times G^{\pi\mathrm{F}}_{\psi^\dagger\psi}$ is reduced as

$$E_1 \times G^{\pi\mathrm{F}}_{\psi^\dagger\psi} = A_1 \oplus A_2 \oplus B_1 \oplus B_2 \oplus A'_1 \oplus A'_2 \oplus B'_1 \oplus B'_2 \oplus 2(E_1 \oplus E'_1 \oplus E_2 \oplus E_3 \oplus E_4 \oplus E_5). \quad (31)$$

The first four irreducible representations which are of interest for us [cf. with Eq. (26)] originate from the E_1 component within $G^{\pi\mathrm{F}}_{\psi^\dagger\psi}$. Consequently, their basis is analogous to Eq. (27). The first four irreducible representations $A_1,\dots,B_2$ from Eq. (31) can be coupled to corresponding irreducible representations in Eq. (26). For example, coupling representation A_1 with basis $k_x\tau^x + k_y\tau^y$ to the A_1 component with basis $u_{xx} + u_{yy}$ results in the contribution

$$\hat{H}^{\pi\mathrm{F}\square}_{\text{s-ph(1)}} = g^{(1)}_{A_1}(u_{xx} + u_{yy})[k_x\tau^x + k_y\tau^y], \quad (32)$$

with a phenomenological coupling constant $g^{(1)}_{A_1}$. Dependence on $\boldsymbol{k},\boldsymbol{q}$ is suppressed for brevity in what follows, $\hat{H}_{\text{s-ph(1)}} \equiv \hat{H}_{\text{s-ph(1)}}(\boldsymbol{k},\boldsymbol{q})$. Collecting all contributions at this order and rearranging phenomenological coupling constants (e.g., $g^{(1)}_{1,4} = g^{(1)}_{A_1} \pm g^{(1)}_{B_1}$), we get the most general form of the spinon-phonon interaction Hamiltonian in the πF phase to be

$$\begin{aligned}\hat{H}^{\pi\mathrm{F}\square}_{\text{s-ph}} = {} & g^{(1)}_1(u_{xx}k_x\tau^x + u_{yy}k_y\tau^y) \\ & + g^{(1)}_2(u_{xy}k_x\tau^x + u_{yx}k_y\tau^y) \\ & + g^{(1)}_3(u_{yx}k_x\tau^x + u_{xy}k_y\tau^y) \\ & + g^{(1)}_4(u_{xx}k_y\tau^y + u_{yy}k_x\tau^x). \end{aligned} \quad (33)$$

C. Results for the sF□, πF✡, and 0F○ phases

After detailed derivation of spinon-phonon interaction for the π-flux phase on a square lattice, we present results for other algebraic spin liquid phases considered in this work.

The staggered-flux phase on a square lattice is similar to the πF□ phase, considered above. However, contrary to the π-flux phase, there is no charge conjugation present among additional symmetries. As we shortly demonstrate, due to reduced symmetry, the number of allowed couplings is going to be larger. Splitting of $G^{\mathrm{sF}\square}_{\psi^\dagger\psi}$ into irreducible components works as

$$G^{\mathrm{sF}\square}_{\psi^\dagger\psi} = A_2 \oplus B_1 \oplus B'_1 \oplus A'_2 \oplus 2E'_1 \oplus 2E_3 \oplus E_4 \oplus E_5. \quad (34)$$

The bases of corresponding components in terms of the tensor product of Pauli matrices are listed in Table II. One can notice that all one-dimensional representations present in the decomposition (34) are odd under time reversal. Just like the case of the πF□ phase, no couplings with phonons are allowed by symmetry at this order. To find nonzero coupling we consider the next order in $\boldsymbol{k}$.

Explicit expression for $\hat{H}_{\text{s-ph(1)}}(\boldsymbol{k})$ can be found using decomposition of the product $E'_1 \times G^{\mathrm{sF}\square}_{\psi^\dagger\psi}$ (where E'_1 corresponds to spinon momentum[32]) into irreducible representations,

$$E'_1 \times G^{\mathrm{sF}\square}_{\psi^\dagger\psi} = 2(A_1 \oplus A_2 \oplus B_1 \oplus B_2 \oplus E_1 \oplus E'_1 \oplus E_2 \oplus E_3 \oplus E_4 \oplus E_5). \quad (35)$$

The overall factor of two indicates that there are two distinct copies of each irreducible representation in the decomposition. Four one-dimensional irreducible representations in the first line of Eq. (35) coincide with the decomposition of $E_1 \times E_1$ into irreducible representations. As all irreducible components are encountered twice in the decomposition (35),

TABLE II. Explicit form of basis for different irreducible representations of C'_{4v} contained within $G^{\mathrm{sF}\square}_{\psi^\dagger\psi}$. The action of the group generators coincides with Ref. 26. The last row summarizes the transformation of basis elements under time-reversal symmetry.

Representation	A_2	B_1	B'_1	A'_2	E'_1	E_3	E_4	E_5
Basis	τ^z	$\tau^z\mu^z$	μ^z	$\mathbb{1}$	$\tau^{x,y},\mu^z\tau^{x,y}$	$\mu^{x,y},\tau^z\mu^{x,y}$	$\mu^{x,y}(\tau^x \mp \tau^y)$	$\mu^{x,y}(\tau^x \pm \tau^y)$
$\mathcal{T}$-inv	$-$	$-$	$-$	$-$	$+$	$+$	$-$	$-$

we have eight different couplings between spinons and phonons.

The basis for the two copies of one-dimensional representations $A_1,\ldots,B_2$ in Eq. (35) can be deduced using the fact that all these irreducible representations originate from the tensor product $E'_1 \times E'_1$:

$$A_1 : k_x\tau^x + k_y\tau^y, \quad A_2 : k_x\tau^y - k_y\tau^x, \tag{36a}$$

$$B_1 : k_x\tau^x - k_y\tau^y, \quad B_2 : k_x\tau^y + k_y\tau^x. \tag{36b}$$

The bases for the second copy of irreducible representations in Eq. (35) have the same form as in Eq. (36), but with an extra Pauli matrix μ^z. Physically, this corresponds to the fact that the anisotropy in Fermi velocity is not prohibited by symmetry in the sF$\square$ phase.[26] Time-reversal invariance does not reduce the number of allowed couplings, as all combinations in Eq. (36) are invariant under $\mathcal{T}$. The resulting spinon-phonon interaction Hamiltonian has eight terms, four of which coincide with the case of the πF$\square$ phase, Eq. (33), while the remaining four terms contain an extra μ^z and correspond to a phonon-induced valley anisotropy in a Fermi velocity.

The π-flux phase on a kagome lattice has a symmetry group C'_{6v}. Just like in the case of square lattice, it is an extension of a conventional symmetry group of a hexagon, C_{6v}, to the case of an enlarged unit cell.[27] The point group of hexagon governs the properties of phonons. The generators of C_{6v} are rotations for an angle of $\pi/3$, $\mathcal{R}_{\pi/3}$, and reflection with respect to the x axis, $\mathcal{R}_x$. Using character Table VIII, the tensor product of two vector representations is decomposed as

$$E_1 \times E_1 = A_1 \oplus A_2 \oplus E_2. \tag{37}$$

On the other hand, using the character table for the group C'_{6v} from Ref. 27, one can reduce representation on fermion bilinears as

$$G^{\pi\mathrm{F}\hexagon}_{\psi^\dagger\psi} = A_1 \oplus A_2 \oplus E_1 \oplus F_1 \oplus F_2 \oplus F_3 \oplus F_4. \tag{38}$$

Comparing Eqs. (37) and (38), we see that, in principle, couplings between corresponding A_1 and A_2 components are possible. However, if we consider properties of representations under time reversal, listed in Table III, we see that the basis of A_2 is odd under time reversal and only coupling to density

TABLE III. Explicit form of basis for irreducible representations of C'_{6v} contained within $G^{\pi\mathrm{F}\hexagon}_{\psi^\dagger\psi}$. Notations and action of group generators coincide with those used by Hermele *et al.*[27]

Representation	A_1	A_2	E_1	F_1	F_2	F_3 and F_4
Basis	$\mathbb{1}$	τ^z	$\tau^{x,y}$	$\tau^z\mu^{x,y,z}$	$\mu^{x,y,z}$	$\tau^{x,y}\mu^{x,y,z}$
$\mathcal{T}$-inv	$+$	$-$	$-$	$+$	$-$	$+$

fluctuations remains:

$$\hat{H}^{\pi\mathrm{F}\hexagon}_{\text{s-ph(0)}} = g^{(0)}_0(u_{xx}+u_{yy})\mathbb{1}. \tag{39}$$

This coupling vanishes for transverse phonon modes, and we consider terms which are next order in $\boldsymbol{k}$. Higher order terms can be found from decomposing of $E_1 \times G^{\pi\mathrm{F}\hexagon}_{\psi^\dagger\psi}$ into irreducible components,

$$E_1 \times G^{\pi\mathrm{F}\hexagon}_{\psi^\dagger\psi} = A_1 \oplus A_2 \oplus 2E_1 \oplus E_2 \oplus 2(F_1 \oplus F_2 \oplus F_3 \oplus F_4), \tag{40}$$

and pairing those with irreducible representations contained within $E_1 \times E_1$, Eq. (37). Only irreducible representations A_1, A_2, and E_2 in Eq. (40) are of interest as the same components are also present in decomposition (37). The basis for these representations can be written in terms of basis of E_1, (k_x,k_y), and the E_1 component within $G^{\pi\mathrm{F}\hexagon}_{\psi^\dagger\psi}$, [$\boldsymbol{\tau} = (\tau^x,\tau^y)$; see Table III]:

$$A_1 : \boldsymbol{k}\cdot\boldsymbol{\tau} \tag{41a}$$

$$A_2 : \boldsymbol{k}\times\boldsymbol{\tau} \tag{41b}$$

$$E_2 : (k_x\tau^y + k_y\tau^x, k_x\tau^x - k_y\tau^y). \tag{41c}$$

From here we can read off the most general form of the spinon-phonon interaction Hamiltonian to be

$$\begin{aligned}\hat{H}^{\pi\mathrm{F}\hexagon}_{\text{s-ph}} = {} & g^{(1)}_1(u_{xx}+u_{yy})(\boldsymbol{k}\cdot\boldsymbol{\tau}) + g^{(1)}_2(u_{xy}-u_{yx})(\boldsymbol{k}\times\boldsymbol{\tau}) \\ & + g^{(1)}_3[(u_{xy}+u_{yx})(k_x\tau^y + k_y\tau^x) \\ & + (u_{xx}-u_{yy})(k_x\tau^x - k_y\tau^y)].\end{aligned} \tag{42}$$

The uniform phase on a honeycomb lattice is also governed by the symmetry group C_{6v}. The notable difference compared to the cases considered above is that the honeycomb lattice is not Bravais and has a unit cell consisting of two atoms. The derivation of spinon-phonon interaction is analogous to the case of graphene.[22] We neglect the optical phonon modes related to the presence of two atoms in the unit cell. The tensor product of two vector representations is given by Eq. (37), whereas decomposition of $G^{0\mathrm{F}\hexagon}_{\psi^\dagger\psi}$ into irreducible representations works as[22]

$$G^{0\mathrm{F}\hexagon}_{\psi^\dagger\psi} = 2(A_1 \oplus A_2 \oplus B_1 \oplus B_2 \oplus E_1 \oplus E_2), \tag{43}$$

where two copies describe matrices diagonal and nondiagonal in valley space. Bases of different irreducible components are given in Table IV. Terms which are off-diagonal in the valley space are not considered, as we do not allow for the intervalley scattering due to phonons. At the zeroth order in $\boldsymbol{k}$, in addition to the density coupling, Eq. (39), there are terms which do not vanish for transverse phonon modes,

$$\hat{H}^{0\mathrm{F}\hexagon}_{\text{s-ph}} = g_1[(u_{xx}-u_{yy})\tau^x - (u_{xy}+u_{yx})\tau^y]\mu^z. \tag{44}$$

TABLE IV. Irreducible representations of C_{6v} contained within $G^{0\mathrm{F}\bigcirc}_{\psi^\dagger\psi}$ and their basis. Each irreducible component occurs twice: The first six representations in the table are diagonal in the valley space, whereas the remaining six are their off-diagonal counterparts. Adapted from Table III in Ref. 22.

Representation	A_1	B_1	A_2	B_2	E_1	E_2	A_1	B_1	A_2	B_2	E_1	E_2
Basis	$\mathbb{1}$	μ^z	τ^z	$\mu^z\tau^z$	$\tau^{x,y}$	$-\mu^z\tau^y, \mu^z\tau^x$	$\mu^x\tau^z$	$\mu^y\tau^z$	μ^x	μ^y	$\mu^x\tau^y, -\mu^x\tau^x$	$\mu^y\tau^{x,y}$
$\mathcal{T}$-inv	$+$	$-$	$-$	$+$	$-$	$+$	$+$	$+$	$-$	$-$	$+$	$+$

Thus, there is no need to consider the next order in $\boldsymbol{k}$. Note that as the basis of A_2 is odd under time reversal, we omit the otherwise possible term $(\partial_x u_y - \partial_y u_x)\tau_z$ from Eq. (44).

D. Comparison between different phases

It is instructive to compare the above results for the spinon-phonon interaction in different realizations of Dirac spin liquid. In all derivations we considered Dirac fermions describing low-energy excitations. The Dirac dispersion arises as an approximation of the band structure in the vicinity of $K_\pm$ points in the Brillouin zone. Consequently, the interaction with acoustic phonons may be understood from the influence of lattice deformations on the low-energy band structure. The coupling of phonons to the density of spinons is very easy to explain from this perspective. The local changes in the volume of the lattice, described exactly by $\mathrm{div}\,\boldsymbol{u} = u_{xx} + u_{yy}$, correspond to the density modulations of spinons, yielding the interaction Hamiltonian (39). In the case of the $0\mathrm{F}\bigcirc$ phase, remaining terms given by Eq. (44) can be interpreted as a relative shift of $K_\pm$ points with respect to each other by lattice deformations. In other words, strain is translated into a gauge field, which coupled with opposite sign in different valleys, which is a well-known effect for the case of graphene.[22,33]

The presence of fluxes and nontrivial action of projective symmetry group prohibits density coupling for $\pi\mathrm{F}\square$ and $\mathrm{sF}\square$ phases. In the $\pi\mathrm{F}\hexagram$ phase, the density coupling is the only allowed coupling at this order. To find nontrivial couplings, we considered next-order expansion in the vicinity of the Dirac points. These couplings may be readily understood as a *deformation* of the band structure in the vicinity of the $K_\pm$ point, which nevertheless leaves the position of the Dirac point within the Brillouin zone intact. This is exactly what we see in couplings (33) and (42), which can be interpreted as the change in Fermi velocity, v_F. Note, that the position of Dirac points in the Brillouin zone is nonuniversal and depends on the choice of the implementation of the given phase. Therefore, it is natural that the (physical) lattice deformation does not have any impact on the (unphysical) position of the Dirac points.

IV. SOUND ATTENUATION

We continue with a discussion of observable consequences of spinon-phonon interaction. The interaction of acoustic phonons with gapless spinons opens additional channel for the decay of phonons. Thus, it is expected to contribute to the attenuation of ultrasound. To get an estimate of the this effect, we perform a simple calculation in this section. As an example, we consider the algebraic spin liquid phase with staggered flux on a square lattice. We comment on the differences for the $\pi\mathrm{F}\hexagram$ and $0\mathrm{F}\bigcirc$ phases. To avoid the complications related to the presence of an SU(2) gauge field we do not consider the $\pi\mathrm{F}\square$ phase.

A. Framework

We start with establishing the framework and introducing the basic elements required to calculate the ultrasound attenuation. These are the gauge field propagator and the phonon self-energy.

The gauge field, strongly coupled to the spinon, emerges from a microscopic constraint and fluctuations around the mean-field ansatz. On a microscopic level it originates from constraint and is not dynamical. Nontrivial dynamics of the gauge field is generated due to the coupling to fermions.[34,35] First, the Maxwell term will be generated while integrating out high-energy degrees of freedom. Another contribution, which is singular compared to the Maxwell term, comes from the Dirac bands touching and can be written via vacuum polarization operator for massless Dirac fermions. The total action of the gauge field then becomes

$$S_a = \frac{1}{2}\int \frac{d^3\vec{q}}{(2\pi)^3} a_\mu(\vec{q})\left[(D^{\mathrm{M}})^{-1}_{\mu\nu}(\vec{q}) - \Pi_{\mu\nu}(\vec{q})\right]a_\nu(-\vec{q}), \quad (45)$$

where we use covariant notations in Euclidean space, $\vec{q} = (i\omega, v_F\boldsymbol{q})$. $\Pi_{\mu\nu}(\vec{q}\,)$ is the polarization bubble of Dirac fermions (see Fig. 2), and $(D^{\mathrm{M}})^{-1}_{\mu\nu}$ is the inverse Maxwell propagator of the gauge field (we work in the Lorentz gauge, $\vec{k}\cdot\vec{a} = 0$),

$$(D^{\mathrm{M}})^{-1}_{\mu\nu}(\vec{q}\,) = \left(\delta_{\mu\nu} - \frac{\vec{q}_\mu \vec{q}_\nu}{\vec{q}^{\,2}}\right)\Pi^{\mathrm{M}}(\vec{q}\,), \quad (46)$$

where $\Pi^{\mathrm{M}}(\vec{q}\,)$ corresponds to the inverse propagator without tensor structure:

$$\Pi^{\mathrm{M}}(\vec{q}\,) = \frac{\vec{q}^{\,2}}{e^2}. \quad (47)$$

The polarization bubble at zero temperature (projector tensor structure is again omitted) is given by[36–38]

$$\Pi(\vec{q}\,) = -\frac{N}{8}\sqrt{\vec{q}^{\,2}}, \quad (48)$$

FIG. 2. Double wavy line shows the gauge field propagator in the RPA approximation. The thin wavy line is the bare Maxwell propagator.

where we introduced the integer number of flavors of four-component Dirac fermions, N, in our theory. The physical case corresponds to $N = 2$ coming from spin. Action (45) translates into the total propagator for the gauge field, Fig. 2, given by

$$D(q) = \frac{8}{N} \frac{1}{\sqrt{\vec{q}^{\,2}} + 8\vec{q}^{\,2}/(Ne^2)}. \tag{49}$$

In what follows we need the polarization bubble at finite temperature, which may be written as

$$\Pi_{\mu\nu} = A_{\mu\nu}\Pi^A + B_{\mu\nu}\Pi^B. \tag{50}$$

The tensors $A_{\mu\nu}$ and $B_{\mu\nu}$,

$$A_{\mu\nu} = \left(\delta_{\mu 0} - \frac{q_\mu q_0}{\vec{q}^{\,2}}\right)\frac{\vec{q}^{\,2}}{\boldsymbol{q}^2}\left(\delta_{0\nu} - \frac{q_0 q_\nu}{\vec{q}^{\,2}}\right), \tag{51}$$

$$B_{\mu\nu} = \delta_{\mu i}\left(\delta_{\mu 0} - \frac{q_\mu q_0}{\vec{q}^{\,2}}\right)\delta_{j\nu}, \tag{52}$$

are orthogonal to each other and their sum reproduces the original zero-temperature tensor structure, Eq. (46). Explicit expressions for $\Pi^{A,B}$ along with detailed calculations are available in the literature.[38] We need the asymptotic expression for Π^A in the limit $T \gg v_F|\boldsymbol{q}| \gg \omega$:

$$\Pi^A = -\frac{2NT\ln 2}{\pi}\left(1 + i\frac{\omega}{v_F q}\right). \tag{53}$$

Sound attenuation, α_s, will be calculated from the self-energy of phonons, $\Pi_{\rm ph}(\omega,\boldsymbol{q})$, arising due to interactions with spinons. More precisely, α_s is given by the imaginary part of the retarded self-energy,[16]

$$\alpha_s = -\frac{2}{v_s}\,\mathrm{Im}\left[\Pi^R_{\rm ph}(\omega,|\boldsymbol{q}|)\right]_{\omega=v_s|\boldsymbol{q}|}, \tag{54}$$

with frequency and momentum related by the dispersion relation of the acoustic phonons, $\omega = v_s|\boldsymbol{q}|$, where v_s is the sound velocity.

Let us discuss the approximations to be used in the calculation of the sound attenuation. For simplicity, we consider the clean case; i.e., we assume that the mean free path of spinons, l, is much larger than the ultrasound wavelength, $ql \gg 1$. Also, we assume that the sound velocity is much smaller than the Fermi velocity, $v_F \gg v_s$. Under this condition, we immediately find that if ω and q are the phonon energy and the wave vector, $v_F q = (v_F/v_s)\omega \gg \omega$. Finally, contrary to the case of spin liquid with a Fermi surface,[16] nonzero temperature is required to get nonvanishing sound attenuation in a Dirac spin liquid. This is a consequence of the energy and momentum conservation in the scattering process. An acoustic phonon cannot excite a particle-hole pair of spinons since the maximum momentum change for such a pair with energy ω, $\Delta k = \omega/v_F$, is much smaller than phonon momentum, $q = \omega/v_s$. Therefore, we assume that the system is at a finite temperature $T \gg (v_F/v_s)\omega \gg \omega$.

As noted above, there is a gauge field strongly coupled to the spinons. In order to have control over its effects we artificially introduced the number of flavors, N, being equal to two in the physical case. Since the gauge field propagator, Eq. (49), is proportional to $1/N$, effects of gauge field are suppressed for large N. We perform calculations of sound attenuation to the leading order within $1/N$ expansion, commenting on the higher order terms.

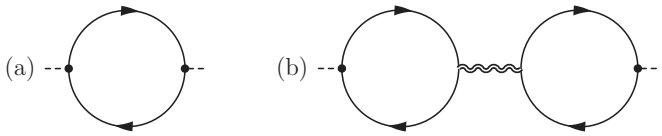

FIG. 3. Contribution of spinons to the longitudinal sound attenuation. The bare contribution from spinons is given by the diagram (a). Diagram (b) accounts for the screening due to fluctuations of the gauge field. Black dots represent spinon-phonon interaction vertexes, specified in the main text.

B. Sound attenuation in the sF□ phase

Having basic ingredients for the calculation of sound attenuation at our disposal, we consider α_s for longitudinal phonons in the sF□ phase. As shown in Sec. III B, there is no allowed coupling at the leading order in $\boldsymbol{k}$. All possible couplings at the next order are given by Eq. (33). For simplicity, we consider only the first term in Eq. (33) [see Eq. (32)]. Combining Eqs. (23) and (32), the corresponding spinon-phonon interaction vertex reads

$$M^{(1)}_{\boldsymbol{k}}(\boldsymbol{q}) = \tilde{g}^{(1)}_1 q\, \tilde{M}^{(1)}_{\boldsymbol{k}}(\hat{\boldsymbol{q}}), \tag{55a}$$

$$\tilde{M}^{(1)}_{\boldsymbol{k}}(\hat{\boldsymbol{q}}) = \hat{q}_x^2 k_x \tau^x + \hat{q}_y^2 k_y \tau^y, \tag{55b}$$

where $\hat{\boldsymbol{q}} = (\hat{q}_x,\hat{q}_y)$ is the unit vector pointing along $\boldsymbol{q}$. In what follows, coupling constants with tildes are defined as

$$\tilde{g} = \sqrt{\frac{1}{2\rho\omega_{\boldsymbol{q}}}}\, g. \tag{56}$$

To leading order in $1/N$, the polarization operator of phonons due to interaction with spinons is given by the sum of two diagrams in Fig. 3 with the spinon-phonon interaction vertex from Eq. (55). Indeed, the first diagram in Fig. 3 has one fermionic bubble and is proportional to N. An extra fermionic bubble in the diagram Fig. 3(b) is compensated by factor of $1/N$ from the gauge field propagator. We have for the first contribution [Fig. 3(a)]:

$$\alpha_s = \frac{2}{v_s}\left[\tilde{g}^{(1)}_1\right]^2 q^2\,\mathrm{Im}\,\Pi^{R(1)}(\omega,\boldsymbol{q}). \tag{57}$$

The imaginary part of the bubble diagram with spinons is calculated in the Appendix B and behaves as $\mathrm{Im}\,\Pi^{R(1)}(\omega,\boldsymbol{q}) \propto N\omega T^3/(v_F^3 q)$ at the leading order. One can show that the contribution from the diagrams with an extra gauge field propagator, Fig. 3(b), has the same order of magnitude as Fig. 3(a). Thus, using a dispersion relation of acoustic phonons, we get the following estimate for the sound attenuation:

$$\alpha_s \propto N\left[\tilde{g}^{(1)}_1\right]^2 \frac{\omega^4 T}{v_s{}^2 v_F^3}. \tag{58}$$

The value of the coupling constant, $g^{(1)}_1$, may be estimated from the sensitivity of the velocity of Dirac spinons to the changes of the lattice constant, a:

$$g^{(1)}_1 \sim a\frac{\partial v_F}{\partial a} \sim v_F. \tag{59}$$

Using this estimate, we obtain for the sound attenuation

$$\alpha_s \sim N \left(\frac{T}{\omega_D}\right)^2 \alpha_s^{(0)}, \tag{60}$$

where $\alpha_s^{(0)}$ is defined as

$$\alpha_s^{(0)} \sim q \frac{k_T}{m_{\text{ion}} v_s} = \frac{qT}{m_{\text{ion}} v_s v_F}. \tag{61}$$

The Debye frequency has been estimated as $\omega_D \propto v_s/a$, and $k_T = T/v_F$ is a wave vector of spinons with the energy equal to the temperature. The $\alpha_s^{(0)}$, introduced above, gives the estimate for the sound attenuation coefficient in the case of spinon Fermi surface if one substitute the Fermi momentum for the $k_T, k_T \to k_F$. We see that in a Dirac spin liquid, contribution of spinons to the sound attenuation is suppressed compared to the Fermi surface case by two factors. The first factor, $T/\mu_F \ll 1$ is generic for any Dirac spin liquid and originates from the vanishing density of states at zero temperature in the Dirac spectrum. The second factor $(T/\omega_D)^2$, which is also expected to be smaller than one, arises due to peculiar form of spinon-phonon coupling.

Finally, we comment on the next order in $1/N$ terms, contributing to the sound attenuation. There is a much larger number of diagrams at the order $O(1)$. The most obvious are the vertex corrections, where gauge field dresses the interaction vertex of spinons with phonons or gauge field itself. Note that if the spinon-phonon interaction vertex corresponded to some conserved current, it would be protected from logarithmic corrections.[35] However, this seems to be not the case here and in general we expect logarithmic corrections to arise at the order $O(1)$. There is also another type of contribution $O(1)$, which is more unusual. Indeed, in order to maintain the gauge invariance, $\boldsymbol{k}$ in Eq. (55) has to be extended to include the gauge field as well. This leads to the vertex where a phonon can generate a quanta of the gauge field *in addition* to the particle-hole pair of spinons. A similar type of vertex has been considered in Ref. 39.

C. Sound attenuation in πF✡ and 0F⬡ phases

As we have shown above, the peculiar form of the coupling between phonons and spinons in the sF□ phase leads to the suppression of the sound attenuation coefficient by additional small factors. One may expect that since in the πF✡ and 0F⬡ phases longitudinal phonons couple to the density of spinons the sound attenuation will be parametrically larger than for the sF□ phase. Below we are going to demonstrate that these naive expectations do not hold. Due to the presence of the gauge field, the density coupling gets screened and does not contribute to the sound attenuation at leading order in $1/N$.

Using an explicit form of the coupling, Eq. (39), we write corresponding spinon-phonon interaction as

$$M_{\boldsymbol{k}}^{(0)}(\boldsymbol{q}) = \tilde{g}_0^{(0)} q \, \mathbb{1}. \tag{62}$$

The identity matrix corresponds to the spinon density, thus justifying the use of the term "density couping." The self-energy of phonons, required to find the sound attenuation, can be expressed via the time component of the electron polarization bubble Π_{00}. In addition, one has to account for the effect of gauge field, including the scalar potential (unlike the case of spinons with Fermi surface, scalar potential of the gauge field is not screened by Dirac fermions). These two contributions to Π_{ph} are shown in Fig. 3, where now black dots correspond to the interaction vertexes (62). Accounting for the both diagrams in Fig. 3, we get

$$\Pi_{\text{ph}}(\vec{q}) = \left[\tilde{g}_0^{(0)}\right]^2 q^2 [\Pi_{00}(\vec{q}) + \Pi_{0\mu}(\vec{q}) D_{\mu\nu}(\vec{q}) \Pi_{\nu 0}(\vec{q})], \tag{63}$$

where propagator and self-energy are taken on a phonon mass shell, $\omega = v_s|\boldsymbol{q}|$. Using the finite-temperature expression for the polarization operator, Eq. (50), we find that only Π^A contributes in the present case. Two terms in the sum in Eq. (63) partially cancel each other and we arrive at

$$\Pi_{\text{ph}}(\vec{q}\,) = \tilde{g}_0^2 q^2 \frac{q^2}{\vec{q}^{\,2}} \frac{\Pi^{\text{M}}(\vec{q}\,)\Pi^A(\vec{q}\,)}{\Pi^{\text{M}}(\vec{q}\,) - \Pi^A(\vec{q}\,)}. \tag{64}$$

Since $\Pi^A(\vec{q}\,)$ is more important than the Maxwell term, at the leading order we can neglect the latter term in the denominator, and get $\Pi_{\text{ph}}(\vec{q}\,) \propto -\Pi^{\text{M}}(q)$. Note that this term is of order of $O(1)$, compared to the naive expectation $\Pi_{\text{ph}}(\vec{q}\,) \sim O(N)$. Moreover, this term does not contribute to the imaginary part of the self-energy: The Maxwell propagator originates from high-energy modes, whereas we are interested in the decay of phonons into low-energy Dirac-like spinons. Omitting the leading order term, and including next order contribution, we get the result

$$\Pi_{\text{ph}}(\vec{q}\,) = -\tilde{g}_0^2 q^2 \frac{q^2}{\vec{q}^{\,2}} \frac{[\Pi^{\text{M}}(\vec{q}\,)]^2}{\Pi^A(\vec{q}\,)}, \tag{65}$$

which is proportional to $1/N$. Qualitatively, cancellation of two leading terms can be understood as an effect of screening due to gauge field.

Now that we have shown that the contribution of the density coupling to the sound attenuation is proportional to $1/N$ and thus negligible, we consider other terms in the coupling Hamiltonian, contributing at the order $O(N)$. For the πF✡ phase, these terms, listed in Eq. (42), are first order in $\boldsymbol{k}$. Thus, the sound attenuation is expected to be of the same order as the results for the sF□ phase, listed in Eq. (60).

However, for the 0F⬡ phase there are couplings allowed without an extra $\boldsymbol{k}$; see Eq. (44). Contribution from these couplings is expected to be of order of $\alpha_s^{(0)}$ [see Eq. (61)]. We note that the contribution of gauge field vanishes in the present case. Indeed, it couples with an opposite sign in different valleys [note the presence of the extra μ^z matrix in Eq. (44)]; thus, the diagram in Fig. 3(b) is identical to zero.

V. DISCUSSION AND OUTLOOK

We presented the general procedure for the derivation of the coupling between spinons and acoustic phonons in the Dirac spin liquid. Our procedure is based on the symmetry arguments. Although a general fermionic bilinear transforms under projective representation of the lattice symmetry group, spin singlet bilinears realize conventional (i.e., not projective) representation of the microscopic symmetry group. We found the decomposition of this representation into irreducible representations for π-flux and staggered-flux phases on a square lattice, as well as for π-flux phase on kagome lattice and a Dirac spin liquid phase on a honeycomb lattice. By

pairing corresponding irreducible representations with those for acoustic phonons, we were able to identify all symmetry-allowed couplings. Note that such decomposition can have other applications. For instance, it can be used to derive symmetry-allowed couplings to optical phonons or some other excitations.

In a continuum limit all considered spin liquid phases have similar low-energy Dirac excitations and hardly can be distinguished. Nevertheless, the allowed interactions with phonons have different form. For the Dirac spin liquid phase on a honeycomb lattice the coupling to acoustic phonons is similar to the case of graphene. The only difference is that the coupling to the density of spinons, naively expected to be the largest, is screened by the gauge field (this is true for all Dirac spin liquid phases). As a result, for spin liquid phases on a square and kagome lattices considered in this work, the leading couplings contains an extra small parameter $(T/\omega_D)^2$, compared to U(1) Dirac spin liquid on honeycomb lattice. Qualitatively, in these phases, the lattice deformations with small wave vectors couple to the changes or anisotropies in Fermi velocity. Whereas in the case of a zero-flux phase on a honeycomb lattice such lattice deformations shift the position of Dirac points, acting similarly to the gauge field.

The difference between couplings arises naturally from the fact that they are controlled by the representation of the corresponding symmetry group, acting on a lattice level. Thus, the interaction of spinons with phonons retains some information about microscopic structure of the phase. It would be instructive to check if one can distinguish between different projective realizations of the same symmetry group by looking at couplings to spinons. The simplest example[40] of such two phases are two $\mathbb{Z}_2$ spin liquid phases on a square lattice (Z2A0013 and Z2Azz13 in notations of Refs. 23 and 41). This, however, requires generalization of the present approach to the case of $\mathbb{Z}_2$ spin liquid phases, which is an interesting open question. Another open question is to understand the effect of projective realization of spin SU(2) symmetry, which has been proposed recently.[42]

In order to understand the perspectives of spinon-phonon interaction as a probe of fermionic spinons, we carried out a simple calculations within $1/N$ expansion. Assuming that our results can be extrapolated to the physical case $N = 2$, we see that the in a generic Dirac spin liquid exemplified by the zero-flux phase in the honeycomb lattice, sound attenuation is suppressed due to vanishing density of states at zero temperature and $\alpha_S \propto qT/(m_{\rm ion} v_F v_s)$. On the other hand, the peculiar form of spinon-phonon coupling in the π-flux and staggered flux phases contributes an additional suppression of the form $(T/\omega_D)^2$. Nevertheless, the effect from phonons is still potentially observable, as the sound attenuation due to phonon-phonon scattering (caused by nonlinearities) behaves as $\alpha \sim T^4$ for $T \ll \omega_D$.[43]

We note that our calculations should be viewed as a simple estimate due to the nature of approximations used. Currently, to the best of our knowledge there are no experimental data available on sound attenuation in Dirac spin liquids. Provided such data becomes available, more extensive theoretical work is required in order to construct a realistic description. In particular, for the prospective spin liquid phase on a kagome lattice,[4,44] the clean limit, assuming mean free path $l \gg q^{-1}$ does not apply. Also, the estimate for v_F suggests that $v_F \sim v_s$, rather than $v_F \gg v_s$, as was assumed. Another question, which can be relevant for a spin liquid on a kagome lattice is the effect of transition from U(1) to $\mathbb{Z}_2$ spin liquid and its possible manifestation in the ultrasound attenuation.

ACKNOWLEDGMENTS

M. S. is grateful to X.-G. Wen, L. Levitov, M. Metlitski, K. Michaeli, K.-T. Chen, and A. Potter for many useful discussions. We acknowledge support by Grant No. NSF DMR 1104498. We acknowledge the hospitality of KITP, where final stages of this project were completed.

APPENDIX A: ELEMENTS OF REPRESENTATION THEORY FOR RELEVANT GROUPS

This Appendix provides background on the representation theory and gives more details for the symmetry groups used in the main text. It starts with a summary of the basic facts from the representation theory of finite groups, which are extensively used throughout the paper. The reader interested in more details or derivations of particular statements is referred to Refs. 45 and 46. Next, the symmetry group of square and its extension, relevant for the πF$\square$ and sF$\square$ phases, is considered. Finally, the basic facts about the symmetry group of hexagon and the symmetry group of the πF$\hexagon$ phase are discussed.

1. Basic facts from representation theory

We consider a point group $\mathcal{G}$, which contains $h_\mathcal{G}$ elements. Notion of conjugacy classes will be of great importance for us in what follows. Conjugacy class is defined as a complete set of mutually conjugate group elements, where two group elements g_1 and g_2 are defined to be conjugate if there exists another group element g_3, such that $g_1 = g_3^{-1} \circ g_2 \circ g_3$. In other words, if g belongs to a given conjugacy class, $\mathcal{C}_i$, then for any group element

$$\forall\, g_j \in \mathcal{G}, \quad g_j^{-1} \circ g \circ g_j \in \mathcal{C}_i, \tag{A1}$$

still is an element from the conjugacy class $\mathcal{C}_i$. Let us assume that the group $\mathcal{G}$ has $n_\mathcal{G}$ conjugacy classes, denoted as $\mathcal{C}_1, \mathcal{C}_2, \ldots, \mathcal{C}_{n_\mathcal{G}}$. Each class contains N_k elements, and, since each group element belongs to only one conjugacy class, we have $\sum_{k=1}^{n_\mathcal{G}} N_k = h_\mathcal{G}$. The identity element, which is necessarily present in any group, is a conjugacy class itself, $\mathcal{C}_1 \equiv E = \{\mathbb{1}\}$ and $N_1 = 1$. For an Abelian group, any element belongs to a separate conjugacy class, so that $n_\mathcal{G} = h_\mathcal{G}$, and $N_{1,\ldots,n_\mathcal{G}} = 1$.

In what follows, our main interest is in classifying representations of a given group. Representation of the group can be thought of as a mapping from the group elements to operators acting on some linear space, $g \to R_g$ which respects the group multiplication, $R_{g_1} \cdot R_{g_2} = R_{g_1 \circ g_2}$. If operators from a given representation cannot be represented as a direct sum of two operators acting on a smaller subspaces, this representation is called irreducible. According to this definition, any representation D can be expressed as a direct sum of irreducible representations,

$$D = a_1 D^{(1)} \oplus a_2 D^{(2)} \oplus \cdots \oplus a_{n_\mathcal{G}} D^{(n_\mathcal{G})}, \tag{A2}$$

where non-negative integers a_i describe how many times a given irreducible representation is encountered in the decomposition. If $D^{(i)}$ is not contained within D, the corresponding a_i is zero, $a_i = 0$. In this way the problem of classifying all representations of a given group is reduced to a classification of all irreducible representations.

The number of different irreducible representations for the group $\mathcal{G}$ coincides with the number of its conjugacy classes, $n_{\mathcal{G}}$. Each irreducible representation, $D^{(i)}$, is specified by the value of its character for different conjugacy classes, defined as

$$\chi^{(i)}(\mathcal{C}_k) = \operatorname{tr} R_{g_{\mathcal{C}_k}}, \quad \text{where} \quad g_{\mathcal{C}_k} \in \mathcal{C}_k. \tag{A3}$$

According to the definition of the conjugacy class (A1), the value of $\chi^{(i)}(\mathcal{C}_k)$ does not depend on the choice of a particular element $g_{\mathcal{C}_k}$ from the $\mathcal{C}_k$. Operators which act on a linear space can be expressed as matrices, and trace in Eq. (A3) is understood in this sense.

The value of character for the conjugacy class which consists of identity $E = \{\mathbb{1}\}$ is special, since it gives us the dimension of the corresponding irreducible representation. To classify all irreducible representations of a given group, it is good to know not only the number of different irreducible representations, but their dimensions as well. In such situation the following relation between the number of elements in the group, $h_{\mathcal{G}}$, and the dimensions of all irreducible representations contained within the group, $\ell_i = \chi^{(i)}(E)$, turns out to be particularly useful:

$$h_{\mathcal{G}} = \sum_{i=1}^{N_{\mathcal{C}}} \ell_i^2. \tag{A4}$$

Typically, only a few sets of integers $\{\ell_1, \ldots, \ell_{N_{\mathcal{G}}}\}$ satisfy this relation, and one can usually identify the correct set of dimensions by involving other considerations.

A character table is a compact way of describing all irreducible representations of a given group. It is a square $n_{\mathcal{G}} \times n_{\mathcal{G}}$ table, where columns correspond to different conjugacy classes, and rows are labeled by different irreducible representations. The entry at an intersection of ith row and jth column is given by the value of the character for the ith representation of the group elements from the jth conjugacy class.

Using the characters table of a given group, one can easily find multiplicities a_i in the decomposition of a representation D into irreducible representations, Eq. (A2). Provided that characters of the representation D, $\chi(\mathcal{C}_k)$, are known, we can find a_i as

$$a_i = \frac{1}{h_{\mathcal{G}}} \sum_{k=1}^{n_{\mathcal{G}}} N_k \, \chi^{(i)*}(\mathcal{C}_k) \, \chi(\mathcal{C}_k), \tag{A5}$$

where $h_{\mathcal{G}}$ is the number of elements in $\mathcal{G}$, and N_k is the number of elements in the corresponding conjugacy class.

If representation D is obtained as the tensor product of two representations, let us say, E and F, $D = E \times F$, the characters of D, $\chi(\mathcal{C}_k) \equiv \chi^{E\times F}(\mathcal{C}_k)$, can be obtained as a product of characters for representations E and F,

$$\chi^{E\times F}(\mathcal{C}_k) = \chi^{E}(\mathcal{C}_k)\chi^{F}(\mathcal{C}_k). \tag{A6}$$

After this, one can easily apply formula (A5) to find the decomposition of the $E \times F$ into irreducible representations.

2. Group of square lattice and its representations

Here we illustrate how the facts summarized above may be used to classify representations of the point symmetry group of square, C_{4v} and its extension, C'_{4v}.

a. Point group of square C_{4v} and its representations

We start with reviewing properties and representations of the point symmetry group of square, C_{4v}. This is the group of all symmetry operations, which leave square invariant. It can be generated by rotations for $\pi/2$ around the center of the square, $\mathcal{R}_{\pi/2}$, and a reflection of the x axis, $\mathcal{R}_x$.[45] In total, the group C_{4v} has $h_{C_{4v}} = 8$ elements. In addition to rotations for angles multiple of $\pi/2$, these include reflections around x and y axes, as well as $\mathcal{R}_{u,v}$, standing for reflections relative to the planes containing vectors $\hat{\boldsymbol{x}} \pm \hat{\boldsymbol{y}}$, $\mathcal{R}_{u,v} = \mathcal{R}_{x,y}\mathcal{R}_{\pi/2}$.

These elements can be split into a total of $n_{C_{4v}} = 5$ conjugacy classes. There are two conjugacy classes consisting of only one group element: trivial $E = \{\mathbb{1}\}$, and $\mathcal{C}_2$ consisting of rotation for π, $\mathcal{C}_2 = \{\mathcal{R}_\pi\}$. Each of the remaining three classes consists of two elements: $\mathcal{C}_4 = \{\mathcal{R}_{\pi/2}, \mathcal{R}_{3\pi/2}\}$, $\mathcal{C}_{xy} = \{\mathcal{R}_x, \mathcal{R}_y\}$, and $\mathcal{C}_{uv} = \{\mathcal{R}_u, \mathcal{R}_v\}$. Correspondingly, group C_{4v} has five irreducible representations. Using Eq. (A4) we find that four of the irreducible representations are one-dimensional and one is a two-dimensional. Characters of these irreducible representations are listed in Table V. One-dimensional representations are fully specified by their list of characters, whereas the two-dimensional representation E_1 corresponds to a transformation of a vector. If we denote the basis of E_1 as $(\hat{\boldsymbol{x}}, \hat{\boldsymbol{y}})$, the action of the group generators becomes

$$\mathcal{R}_{\pi/2}: \quad \hat{\boldsymbol{x}} \to \hat{\boldsymbol{y}}, \quad \hat{\boldsymbol{y}} \to -\hat{\boldsymbol{x}}, \tag{A7a}$$

$$\mathcal{R}_{x}: \quad \hat{\boldsymbol{x}} \to -\hat{\boldsymbol{x}}, \quad \hat{\boldsymbol{y}} \to \hat{\boldsymbol{y}}. \tag{A7b}$$

Using Table V we can easily find decomposition of the Kronecker product of $E_1 \times E_1$ into irreducible representations.[45] Only two nonzero characters of $E_1 \times E_1$ are $\chi^{E_1\times E_1}(E) = \chi^{E_1\times E_1}(\mathcal{C}_2) = 4$. Now, using Eq. (A5) we can find that the first four representations in Table V are contained once within $E_1 \times E_1$: Corresponding multiplicities are all equal to one, $a_i = 1/8 \cdot (4 + 4) = 1$. Whereas for E_1, we find the corresponding a to be zero. This may be summarized as

$$E_1 \times E_1 = A_1 \oplus A_2 \oplus B_1 \oplus B_2. \tag{A8}$$

Although formula (A5) gives us information about representations contained within $E_1 \times E_1$, it does not give explicit expression for the basis of these irreducible representations.

TABLE V. Irreducible representations of C_{4v} and their characters.

Representations	E	$\mathcal{C}_2$	$\mathcal{C}_4$	$\mathcal{C}_{xy}$	σ_{uv}
A_1	1	1	1	1	1
A_2	1	1	1	−1	−1
B_1	1	1	−1	1	−1
B_1	1	1	−1	−1	1
E_1	2	−2	0	0	0

In the present case the explicit form of the basis may be easily guessed from physical arguments. Basis of each E_1 in the product can be written as a two components of a vector, with the action of generators specified in Eq. (A7). Having components of two vectors (q_x,q_y) and (u_x,u_y), one can easily guess that the quantity, invariant under all symmetries, is the scalar product. Thus, $\boldsymbol{q}\cdot\boldsymbol{u} = q_x u_x + q_y u_y$ is a basis of the A_1 component, contained in Eq. (A8). The basis for A_2 is also easy to guess, as it has to change sign under any reflection. Thus, it is given by the vector product, $\boldsymbol{q}\times\boldsymbol{u} = q_x u_y - q_y u_x$. Finally, one can check that remaining combinations $q_x u_x - q_y u_y$ and $q_x u_y + q_y u_x$ realize the basis for B_1 and B_2 irreducible representations. This leads us to Eq. (27) in the main text, which summarizes the above results.

b. Group C'_{4v} and its representations

From the group C_{4v} we move to the group $C'_{4v} = G_\square/G_{2t}$, which is the factor group of the space group of square lattice $G_\square$ over the group of translations for two unit cell vectors G_{2t}. In other words, group C'_{4v} is defined as group C_{4v} with added translation operations $t_{\boldsymbol{a}_1}$ and $t_{\boldsymbol{a}_2}$. In order to specify this group we use Seitz operators $\{R|\boldsymbol{t}\}$ defined as

$$\{R|\boldsymbol{t}\}\cdot\boldsymbol{r} = R\cdot\boldsymbol{r} + \boldsymbol{t}. \tag{A9}$$

The group

$$G_t = \{\{\mathbb{1}|0\},\{\mathbb{1}|\boldsymbol{a}_1\},\{\mathbb{1}|\boldsymbol{a}_2\},\{\mathbb{1}|\boldsymbol{a}_1+\boldsymbol{a}_2\}\} \tag{A10}$$

is the subgroup of C'_{4v} and it contains $h_{G_t} = 4$ elements. The group C'_{4v} has $h_{C'_{4v}} = h_{G_t}\cdot h_{4v} = 32$ elements. It has $n_{C'_{4v}} = 14$ conjugacy classes, which are listed in Table VI.

Representations of C'_{4v} can be worked out using the fact that it has a subgroup G_t. Consequently, we can easily obtain five irreducible representations, one-dimensional $A_{1,2}$ and $B_{1,2}$ along with two-dimensional E_1, from corresponding irreducible representations of C_{4v}. For this we simply assume the action of translations to be trivial. Assuming that translation results in multiplying basis elements by minus one, we find an additional four one-dimensional irreducible representations, denoted as $A'_{1,2}$ and $B'_{1,2}$, to emphasize that these are an extension of corresponding representations from C_{4v}. An analogous extension of E_1 is denoted as E'_1. The remaining four two-dimensional irreducible representations can be found explicitly using SU(4) generators given by $\{\mu^i,\tau^i,\mu^i\tau^j\}$ as a basis. The action of translations for representations $E_2,\ldots,E_5$ can be written as

$$T_{x,y}:\ \ \hat{\boldsymbol{x}}\to\mp\hat{\boldsymbol{x}},\quad \hat{\boldsymbol{y}}\to\pm\hat{\boldsymbol{y}}, \tag{A11}$$

so that $T_xT_y = -\mathbb{1}$. However, the transformation of basis under rotation and reflection are realized differently for each of these representations. For representations E_2 and E_3 we have

$$\mathcal{R}_{\pi/2}:\ \ \hat{\boldsymbol{x}}\to\hat{\boldsymbol{y}},\quad \hat{\boldsymbol{y}}\to\hat{\boldsymbol{x}}, \tag{A12a}$$

$$\mathcal{R}_{x}:\ \ \hat{\boldsymbol{x}}\to\mp\hat{\boldsymbol{x}},\quad \hat{\boldsymbol{y}}\to\mp\hat{\boldsymbol{y}}, \tag{A12b}$$

with the minus (plus) sign corresponding to E_2 (E_3). For E_4 (E_5) we get

$$\mathcal{R}_{\pi/2}:\ \ \hat{\boldsymbol{x}}\to\mp\hat{\boldsymbol{y}},\quad \hat{\boldsymbol{y}}\to\pm\hat{\boldsymbol{x}}, \tag{A13a}$$

$$\mathcal{R}_{x}:\ \ \hat{\boldsymbol{x}}\to\mp\hat{\boldsymbol{x}},\quad \hat{\boldsymbol{y}}\to\pm\hat{\boldsymbol{y}}. \tag{A13b}$$

The character table may be easily calculated from here, and it is summarized in Table VII.

From characters we determine the decomposition of different representations of C'_{4v} on fermion bilinears into irreducible representations. Indeed, the basis in the space of all possible fermion bilinears that are singlets in spin sector can be constructed using SU(4) generators $\{\mu^i,\tau^i,\mu^i\tau^j\}$. Therefore, this problem is equivalent to reducing adjoint representation of C'_{4v} on 16 4×4 matrices $\{\mathbb{1},\mu^i,\tau^i,\mu^i\tau^j\}$. Representation is fully specified by the action of generators. For the cases of the πF$\square$ phase these are given by Eqs. (13)–(19), whereas for the sF$\square$ phase the reader is referred to Ref. 26. (Note that there $\mathcal{R}_x$ is defined as a reflection with respect to the edge of square, whereas in our conventions reflection plane goes through the center of the plaquette. Therefore, $\mathcal{R}_x$ from Ref. 26 coincides with $T_x\mathcal{R}_x$ in our notations.) Calculating characters and applying Eq. (A5), we find

$$G^{\pi\mathrm{F}\square}_{\psi^\dagger\psi} = A_1\oplus A_2\oplus B'_1\oplus B'_2\oplus E_1\oplus E'_1 \oplus E_2\oplus E_3\oplus E_4\oplus E_5 \tag{A14}$$

for the πF$\square$ phase, where basis in terms of products of Pauli matrices for each irreducible componentis listed in Table I in the main text. We also obtained the same expressions for bases of different representations using the notations from Ref. 25. Analogously, for the πF$\square$ phase we have

$$G^{\mathrm{sF}\square}_{\psi^\dagger\psi} = A_2\oplus B_1\oplus B'_1\oplus A'_2\oplus 2E'_1\oplus 2E_3\oplus E_4\oplus E_5, \tag{A15}$$

with details on the basis listed in Table II. From here we immediately recover the result of Refs. 25 and 26 that no invariant fermion bilinear terms exist in πF$\square$ and sF$\square$ phases.

TABLE VI. Labeling of conjugacy classes of group C'_{4v}. Below each label, the number of group elements, $N_{\mathcal{C}}$, belonging to a given conjugacy class, as well as explicit form of these elements in Seitz notations, are given. Vector $\boldsymbol{a}_3$ is a short-hand notation for the sum of lattice vectors, $\boldsymbol{a}_3 = \boldsymbol{a}_1+\boldsymbol{a}_2$.

Conjugacy class	E	$\mathcal{C}_t$	$\mathcal{C}_{tt}$	$\mathcal{C}_2$	$\mathcal{C}_{2t}$	$\mathcal{C}_{2tt}$	$\mathcal{C}_4$
$N_{\mathcal{C}}$	1	2	1	1	2	1	4
Members	$\mathbb{1}$	$\{\mathbb{1}\|\boldsymbol{a}_{1,2}\}$	$\{\mathbb{1}\|\boldsymbol{a}_3\}$	$\{\mathcal{R}_\pi\|0\}$	$\{\mathcal{R}_\pi\|\boldsymbol{a}_{1,2}\}$	$\{\mathcal{R}_\pi\|\boldsymbol{a}_3\}$	$\{\mathcal{R}^{1,3}_{\pi/2}\|0,\boldsymbol{a}_3\}$
Conjugacy class	$\mathcal{C}_{4t}$	$\mathcal{C}_{xy}$	$\mathcal{C}_{xyt_1}$	$\mathcal{C}_{xyt_2}$	$\mathcal{C}_{xytt}$	$\mathcal{C}_{uv}$	$\mathcal{C}_{uvt}$
$N_{\mathcal{C}}$	4	2	2	2	2	4	4
Members	$\{\mathcal{R}^{1,3}_{\pi/2}\|\boldsymbol{a}_{1,2}\}$	$\{\mathcal{R}_{x,y}\|0\}$	$\{\mathcal{R}_x\|\boldsymbol{a}_1\}$ $\{\mathcal{R}_y\|\boldsymbol{a}_2\}$	$\{\mathcal{R}_x\|\boldsymbol{a}_2\}$ $\{\mathcal{R}_y\|\boldsymbol{a}_1\}$	$\{\mathcal{R}_{x,y}\|\boldsymbol{a}_3\}$	$\{\mathcal{R}_{u,v}\|0,\boldsymbol{a}_3\}$	$\{\mathcal{R}_{u,v}\|\boldsymbol{a}_{1,2}\}$

TABLE VII. Irreducible representations of C'_{4v} and their characters. The first eight representations are one-dimensional; the remaining six representations are two-dimensional.

Representation	E	$\mathcal{C}_t$	$\mathcal{C}_{tt}$	$\mathcal{C}_2$	$\mathcal{C}_{2t}$	$\mathcal{C}_{2tt}$	$\mathcal{C}_4$	$\mathcal{C}_{4t}$	$\mathcal{C}_{xy}$	$\mathcal{C}_{xyt_1}$	$\mathcal{C}_{xyt_2}$	$\mathcal{C}_{xytt}$	$\mathcal{C}_{uv}$	$\mathcal{C}_{uvt}$
A_1	1	1	1	1	1	1	1	1	1	1	1	1	1	1
A_2	1	1	1	1	1	1	1	1	−1	−1	−1	−1	−1	−1
B_1	1	1	1	1	1	1	−1	−1	1	1	1	1	−1	−1
B_2	1	1	1	1	1	1	−1	−1	−1	−1	−1	−1	1	1
A'_1	1	−1	1	1	−1	1	1	−1	1	−1	−1	1	1	−1
A'_2	1	−1	1	1	−1	1	1	−1	−1	1	1	−1	−1	1
B'_1	1	−1	1	1	−1	1	−1	1	1	−1	−1	1	−1	1
B'_2	1	−1	1	1	−1	1	−1	1	−1	1	1	−1	1	−1
E_1	2	2	2	−2	−2	−2	0	0	0	0	0	0	0	0
E'_1	2	−2	2	−2	2	−2	0	0	0	0	0	0	0	0
E_2	2	0	−2	2	0	−2	0	0	−2	0	0	2	0	0
E_3	2	0	−2	2	0	−2	0	0	2	0	0	−2	0	0
E_4	2	0	−2	−2	0	2	0	0	0	2	−2	0	0	0
E_5	2	0	−2	−2	0	2	0	0	0	−2	2	0	0	0

Indeed, $G^{\mathrm{sF}\square}$ does not contain trivial representation A_1. Whereas even though $G^{\pi\mathrm{F}\square}$ contains A_1, as one can see from Table I it is not invariant under time reversal, $\mathcal{T}$, nor under charge conjugation, $\mathcal{C}$.

3. Group of honeycomb and kagome lattices

Since an extensive details for kagome and honeycomb lattices are available in the literature,[22,27] we only briefly summarize the basic facts for the symmetry group of the hexagon C_{6v} and its extension for the $\pi\mathrm{F}\hexagram$ phase. More details for the honeycomb lattice can be found in Ref. 22.

a. Point group of hexagon

For kagome and honeycomb lattices the relevant point group is that of a hexagon, denoted as C_{6v}. It has $h_{C_{6v}} = 12$ elements and can be generated by the rotation $\mathcal{R}_{\pi/3}$ and the reflection of the y axis, $\mathcal{R}_y$. It has six different conjugacy classes and six irreducible representations, of which four are one-dimensional and the remaining ones are two-dimensional. Using characters of C_{6v} shown in Table VIII, we can write the product of $E_1 \times E_1$ as

$$E_1 \times E_1 = A_1 \oplus A_2 \oplus E_2. \tag{A16}$$

b. C'_{6v} for kagome lattice

The ansatz for the algebraic spin liquid on Kagome lattice has a larger unit cell than the case without any fluxes. Thus, to classify fermionic bilinears, we again have to consider enlarged group, C'_{6v}, which is the C_{6v} with added translations for primitive lattice vectors $\boldsymbol{a}_1$ and $\boldsymbol{a}_2$.

TABLE VIII. Irreducible representations of the group C_{6v} and their characters.

Representation	E	$\mathcal{C}_2$	$\mathcal{C}_3$	$\mathcal{C}_6$	$\mathcal{C}_a$	$\mathcal{C}_{a'}$
A_1	1	1	1	1	1	1
A_2	1	1	1	1	−1	−1
B_2	1	−1	1	−1	1	−1
B_1	1	−1	1	−1	−1	1
E_1	2	−2	−1	1	0	0
E_2	2	2	−1	−1	0	0

The group C'_{6v} (or, G_{s2} in notations of Ref. 27) has been studied extensively and its conjugacy classes along with characters are listed in Tables III and IV in Ref. 27. Using this information, we may find the decomposition of the representation on bilinears as in Eq. (38) with bases of corresponding irreducible components listed in Table III.

In the next order, we have to decompose the $E_1 \times G^{\pi\mathrm{F}\hexagram}_{\psi^\dagger\psi}$ into irreducible representations. This leads us to Eq. (40) in the main text, where components A_1, A_2, and E_2, which are of interest for us originate from the tensor product of E_1 with another E_1, contained within Eq. (38). This readily allows us to find the basis for these representations.

APPENDIX B: CALCULATION OF THE POLARIZATION OPERATOR

In this Appendix we calculate the imaginary part of the polarization bubble. We work using assumptions, specified in the main text. In particular, we restrict ourselves to the clean limit $ql \gg 1$ and assume the temperature to be the largest energy scale in the problem, $T \gg v_F q \gg \omega$. Note that we use the explicit value of $N = 2$ corresponding to spin. Since the polarization operator is proportional to N, one can easily restore the answer for the general case.

We write the polarization operator, $\Pi^{(i)}$, corresponding to the interaction vertex $\tilde{M}^{(i)}(\hat{\boldsymbol{q}})$ as

$$\mathrm{Im}\,\Pi^{(i)}(i\omega_n, \boldsymbol{q}) = 2T\,\mathrm{Im}\int (dk) \sum_m \mathrm{tr}\left[\tilde{M}^{(i)}_{\boldsymbol{k}}(\hat{\boldsymbol{q}}) G_{\boldsymbol{k}+\boldsymbol{q}} \times (i\omega_m + i\omega_n)\tilde{M}^{(i)}_{\boldsymbol{k}+\boldsymbol{q}}(\hat{\boldsymbol{q}}) G_{\boldsymbol{k}}(i\omega_m)\right], \tag{B1}$$

where $(dk) = dk_x dk_y/(2\pi)^2$ is the short-hand notation for the momentum integration measure. The interaction vertex $\tilde{M}^{(i)}(\hat{\boldsymbol{q}})$, as well as the Green's function, are matrices in spinor space, and the tracing in (B1) goes over matrix indices. After analytical continuation, the imaginary part of the Matsubara

sum of two Green's functions is written as

$$\mathrm{Im}\sum_m [G_{\boldsymbol{k}+\boldsymbol{q}}(i\omega_m+i\omega_n)]_{\alpha\beta}[G_{\boldsymbol{k}}(i\omega_m)]_{\gamma\delta} = \frac{1}{2\pi T}\int dz \left(\tanh\frac{z}{2T}-\tanh\frac{z+\omega}{2T}\right) \times \mathrm{Im}\left[G^R_{\boldsymbol{k}+\boldsymbol{q}}(z+\omega)\right]_{\alpha\beta}\mathrm{Im}\left[G^A_{\boldsymbol{k}}(z)\right]_{\gamma\delta}, \quad \text{(B2)}$$

where we restored internal indices. $G^{R,A}_{\boldsymbol{k}}(z)$ stands for retarded (advanced) Green's function for real frequencies,

$$G^{R,A}_{\boldsymbol{k}}(z,\boldsymbol{k}) = \frac{z+v_F\boldsymbol{\tau}\cdot\boldsymbol{k}}{(z\pm i0)^2-v_F^2\boldsymbol{k}^2}. \quad \text{(B3)}$$

In what follows, we need the expression for the trace of numerators of two Green's functions with corresponding interaction vertices in Eq. (B1). For the case of density coupling, defined in Eq (62), we have $\tilde{M}^{(0)}_{\boldsymbol{k}}(\hat{\boldsymbol{q}}) = \mathbb{1}$, and the trace is evaluated as

$$T^{(0)}(z,\omega,\boldsymbol{k},\boldsymbol{q}) = \mathrm{tr}[\mathbb{1}\cdot(z+\omega+v_F\boldsymbol{\tau}\cdot(\boldsymbol{k}+\boldsymbol{q}))\cdot\mathbb{1}\cdot(z+v_F\boldsymbol{\tau}\cdot\boldsymbol{k})] = 4\left[(z+\omega)z+(v_Fk)^2+v_F^2kq\cos\theta\right], \quad \text{(B4)}$$

with θ being the angle between vectors $\boldsymbol{k}$ and $\boldsymbol{q}$. Note that there is an additional factor of two in (B4) from accounting for the (trivial) valley structure, whereas the factor of two originating from spin degrees of freedom is included in Eq. (B1). For the case of spinon-phonon coupling, arising in the next order of expansion in $\boldsymbol{k}$, the $\tilde{M}^{(1)}_{\boldsymbol{k}}(\hat{\boldsymbol{q}})$ is given by Eq. (55b) and the trace results in a cumbersome expression for $T^{(1)}(z,\omega,\boldsymbol{k},\boldsymbol{q})$, which will be not listed here. Using the expression for the imaginary part of Green's functions, we have

$$\mathrm{Im}\,\Pi^{R(i)}(\omega,\boldsymbol{q}) = \pi\,\mathrm{Im}\int(dk)\int dz\left(\tanh\frac{z}{2T}-\tanh\frac{z+\omega}{2T}\right)T^{(i)}(z,\omega,\boldsymbol{k},\boldsymbol{q})\frac{1}{4v_Fk}\left[\frac{\delta(z+v_Fk)\delta(\omega+v_Fk'-v_Fk)}{v_Fk-\omega}\right. + \frac{\delta(z-v_Fk)\delta(\omega-v_Fk'+v_Fk)}{v_Fk+\omega} + \frac{\delta(z+v_Fk)\delta(\omega-v_Fk'-v_Fk)}{v_Fk-\omega} + \left.\frac{\delta(z-v_Fk)\delta(\omega+v_Fk'+v_Fk)}{v_Fk+\omega}\right]. \quad \text{(B5)}$$

We drop last two terms in the square brackets since they correspond to interband transitions, and for $\omega \ll v_Fq$ they are not important. Also, we expand the difference between hyperbolic tangents, thus getting the derivative of the Fermi distribution function, denoted as $n'_F(z)$:

$$\mathrm{Im}\,\Pi^{R(i)}(\omega,\boldsymbol{q}) = 2\pi\omega\int(dk)\int dz n'_F(z)T^{(i)}(z,\omega,\boldsymbol{k},\boldsymbol{q})\frac{1}{4v_Fk}\left[\frac{\delta(z+v_Fk)\delta(\omega+v_Fk'-v_Fk)}{v_Fk-\omega}+\frac{\delta(z-v_Fk)\delta(\omega-v_Fk'+v_Fk)}{v_Fk+\omega}\right]. \quad \text{(B6)}$$

Using δ functions, we may get rid of the integration over z. An integral over angle between vectors $\boldsymbol{k}$ and $\boldsymbol{q}$, denoted as θ, can be done using the following expression:

$$\int d\theta\,\delta(\pm\omega - v_F|\boldsymbol{k}+\boldsymbol{q}|+v_Fk)F(\theta) = 2\theta(2k-q)\frac{v_Fk\pm\omega}{v_0^2kq|\sin\theta_0^\pm|}F(\theta_0^\pm), \quad \text{where} \quad \cos\theta_0^\pm = \frac{\omega^2}{2v_F^2kq}\pm\frac{\omega}{v_Fq}-\frac{q}{2k}. \quad \text{(B7)}$$

This is valid in the limit when $v_Fq \gg \omega$. Note, that we included an extra factor 2 to account for two possible values of θ_0^+ (and θ_0^-), assuming that the $F(\theta_0^+)$ is the same for both solutions. The integration over θ in Eq. (B6) yields

$$\mathrm{Im}\,\Pi^{R(i)}(\omega,\boldsymbol{q}) = \frac{\omega}{4\pi v_0^3q}\int_{q/2}^\infty dk\left[n'_F(-v_Fk)\frac{T^{(i)}(-v_Fk,\omega,\boldsymbol{k},\boldsymbol{q})|_{\theta=\theta_0^-}}{k|\sin\theta_0^-|} + n'_F(v_Fk)\frac{T^{(i)}(v_Fk,\omega,\boldsymbol{k},\boldsymbol{q})|_{\theta=\theta_0^+}}{k|\sin\theta_0^+|}\right]. \quad \text{(B8)}$$

We notice, that expression in the square brackets in Eq. (B8) does not vanish if we put ω to zero within it for the case of density coupling [when $T(z,k,\theta)$ is given by Eq. (B4)]. In this case, accounting for the fact that $n'_F(v_Fk)$ for the vanishing chemical potential is an even function, we have

$$\mathrm{Im}\,\Pi^{R(0)}(\omega,\boldsymbol{q}) = \frac{4\omega}{\pi v_Fq}\int_{q/2}^\infty dk\,n'_F(v_Fk)\sqrt{k^2-(q/2)^2} = -\frac{4\omega}{\pi v_Fq}T\ln 2. \quad \text{(B9)}$$

When calculating the integral we used the fact that the main contribution to the integral comes from $v_Fk \sim T$; thus, we may neglect by q in the square root. This answer reproduces the results, available in the literature.[36–38,47,48] Recalling that this polarization operator is proportional to N, which was assumed to be $N = 2$ for this calculation, we reproduce the imaginary part of the result listed in the main text, Eq. (53).

The calculation for the case of the next order coupling, $\tilde{M}^{(1)}_{\boldsymbol{k}}(\hat{\boldsymbol{q}})$, requires more care. The answer depends on the direction of the phonon momentum, $\boldsymbol{q}$. We define the ϕ to be an angle of $\boldsymbol{q}$ relative to the x axis, so that $\hat{\boldsymbol{q}} = (\cos\phi,\sin\phi)$. Lengthy but straightforward calculation gives for the polarization operator in this case:

$$\mathrm{Im}\,\Pi^{R(1)}(\omega,\boldsymbol{q}) = \frac{\omega\sin^4 2\phi}{\pi q}\int_{q/2}^\infty dk\,n'_F(v_Fk)\frac{k^4}{\sqrt{k^2-(q/2)^2}} = -\frac{9\zeta(3)}{2\pi}\frac{\omega}{v_F^3q}T^3\sin^4 2\phi. \quad \text{(B10)}$$

It is noteworthy that the answer is invariant under rotations of $\pi/2$, as one may expect for our case. The angular dependence of (B10) is very anisotropic; in particular, when $\boldsymbol{q}$ points along x or y axis, the results vanish, indicating that the answer will be of higher order in ω.

[1] P. W. Anderson, Mater. Res. Bull. **8**, 153 (1973); Science **235**, 1196 (1987).
[2] P. A. Lee, Science **321**, 1306 (2008).
[3] L. Balents, Nature (London) **464**, 199 (2010).
[4] T.-H. Han, J. S. Helton, S. Chu, D. G. Nocera, J. A. Rodriguez-Rivera, C. Broholm, and Y. S. Lee, Nature **492**, 406 (2012).
[5] P. A. Lee and N. Nagaosa, Phys. Rev. B **87**, 064423 (2013).
[6] W.-H. Ko, Z.-X. Liu, T.-K. Ng, and P. A. Lee, Phys. Rev. B **81**, 024414 (2010).
[7] W.-H. Ko and P. A. Lee, Phys. Rev. B **84**, 125102 (2011).
[8] D. F. Mross and T. Senthil, Phys. Rev. B **84**, 041102 (2011).
[9] O. A. Starykh and L. Balents, Phys. Rev. Lett. **98**, 077205 (2007).
[10] K.-S. Kim and M. D. Kim, J. Phys.: Condens. Matter **20**, 125206 (2008).
[11] P. Ribeiro and P. A. Lee, Phys. Rev. B **83**, 235119 (2011).
[12] M. Serbyn, T. Senthil, and P. A. Lee, arXiv:1212.5179.
[13] A. C. Potter, T. Senthil, and P. A. Lee, arXiv:1301.3495.
[14] D. V. Pilon, C. H. Lui, T. Han, D. B. Shrekenhamer, A. J. Frenzel, W. J. Padilla, Y. S. Lee, and N. Gedik, arXiv:1301.3501.
[15] Also, optical phonons have been suggested as a possible means for detection of VBS order in Ref. 27.
[16] Y. Zhou and P. A. Lee, Phys. Rev. Lett. **106**, 056402 (2011).
[17] E. I. Blount, Phys. Rev. **114**, 418 (1959).
[18] T. Tsuneto, Phys. Rev. **121**, 402 (1961).
[19] S. Rodriguez and E. Kartheuser, Superlattices Microstruct. **1**, 503 (1985).
[20] F. S. Khan and P. B. Allen, Phys. Rev. B **29**, 3341 (1984).
[21] J. L. Mañes, Phys. Rev. B **76**, 045430 (2007).
[22] D. M. Basko, Phys. Rev. B **78**, 125418 (2008).
[23] X.-G. Wen, Phys. Rev. B **65**, 165113 (2002).
[24] X. Wen, *Quantum Field Theory of Many-Body Systems:From the Origin of Sound to an Origin of Light and Electrons* (Oxford University Press, Oxford, 2004).
[25] M. Hermele, T. Senthil, M. P. A. Fisher, P. A. Lee, N. Nagaosa, and X.-G. Wen, Phys. Rev. B **70**, 214437 (2004).
[26] M. Hermele, T. Senthil, and M. P. A. Fisher, Phys. Rev. B **72**, 104404 (2005).
[27] M. Hermele, Y. Ran, P. A. Lee, and X.-G. Wen, Phys. Rev. B **77**, 224413 (2008).
[28] W. Rantner and X.-G. Wen, Phys. Rev. Lett. **86**, 3871 (2001).
[29] W. Rantner and X.-G. Wen, Phys. Rev. B **66**, 144501 (2002).
[30] O. Vafek, Z. Tešanović, and M. Franz, Phys. Rev. Lett. **89**, 157003 (2002).
[31] M. Franz, Z. Tešanović, and O. Vafek, Phys. Rev. B **66**, 054535 (2002).
[32] Naively, the fact that $\boldsymbol{k}$ transforms under E_1' rather than E_1 seems to contradict the expectation, that as the staggered flux becomes exactly equal to π the sF$\square$ phase continuously evolves into the πF$\square$ phase. In reality, there is no contradiction: The sF$\square$ phase at the value of flux of π indeed turns into the πF$\square$ phase; however, it is realized with a different ansatz.
[33] M. Vozmediano, M. Katsnelson, and F. Guinea, Phys. Rep. **496**, 109 (2010).
[34] L. B. Ioffe and A. I. Larkin, Phys. Rev. B **39**, 8988 (1989).
[35] D. H. Kim and P. A. Lee, Ann. Phys. **272**, 130 (1999).
[36] N. Dorey and N. E. Mavromatos, Nucl. Phys. B **386**, 614 (1992).
[37] D. V. Khveshchenko, Phys. Rev. B **74**, 161402 (2006).
[38] O. Vafek, Ph.D. thesis, Johns Hopkins University, Baltimore, MD, 2003.
[39] Y. B. Kim, A. Furusaki, X.-G. Wen, and P. A. Lee, Phys. Rev. B **50**, 17917 (1994).
[40] X.-G. Wen (private communication).
[41] X.-G. Wen, Quantum Orders and Symmetric Spin Liquids (The Original Version) (2001), http://dao.mit.edu/∼wen/pub/qosl.pdf.
[42] G. Chen, A. Essin, and M. Hermele, Phys. Rev. B **85**, 094418 (2012).
[43] T. O. Woodruff and H. Ehrenreich, Phys. Rev. **123**, 1553 (1961).
[44] J. S. Helton, K. Matan, M. P. Shores, E. A. Nytko, B. M. Bartlett, Y. Yoshida, Y. Takano, A. Suslov, Y. Qiu, J.-H. Chung, D. G. Nocera, and Y. S. Lee, Phys. Rev. Lett. **98**, 107204 (2007).
[45] M. Hamermesh, *Group Theory and its Application to Physical Group Theory and Its Application to Physical Problems*, Addison-Wesley Series in Physics (Addison-Wesley, Reading, MA, 1962).
[46] F. Porter, Notes on Representation Theory, http://www.hep.caltech.edu/∼fcp/math/groupTheory/represen.pdf.
[47] B. Wunsch, T. Stauber, F. Sols, and F. Guinea, New J. Phys. **8**, 318 (2006).
[48] E. H. Hwang and S. Das Sarma, Phys. Rev. B **75**, 205418 (2007).